CEAS Aeronautical Journal manuscript No.
(will be inserted by the editor)

Aircraft Noise Generation and Assessment

Combustion Noise: Modeling and Prediction

C. K. W. Tam · F. Bake · L. S. Hultgren · T. Poinsot

August 21, 2018

Abstract This paper reviews both direct and indirect combustion noise. For convenience, they will simply be referred to as combustion noise and entropy noise. Combustion noise has been studied for well over half a century. However, because of the large number of parameters involved and the complexities inherent in the combustion processes, a widely accepted theory has yet to be developed. For this reason, this review focuses primarily on experimental measurements, semi-empirical relations and empirical but practical prediction methodologies. Important characteristic features and empirical correlations of combustion noise based on open flames and engine noise data are highlighted. Plausible generation of entropy noise by the passage of entropy waves through a nonuniform mean flow was first predicted theoretically circa 1970s. But it took forty years for its existence to be confirmed experimentally. Since then, there have been numerous publications on this subject. They are the primary materials of this review. The fundamental experiment and noise generation mechanism will be discussed first. Of great practical importance is whether there is significant generation of entropy waves inside an engine. This issue and new methods for modeling and predicting internally generated engine entropy noise are items that are examined at some length. Recent advances in computational methods especially in large eddy simulation lead us to envision an important role to be played by high-fidelity numerical simulation in future combustion and entropy noise research and prediction. A critical evaluation of a strategy for investigating and predicting the generation and propagation of these noise components from the combustor of an engine to its exhaust is included in this review.

Keywords aeroacoustics · propulsion noise · combustion noise · modeling · prediction

C. K. W. Tam
Florida State University, USA
E-mail: tam@math.fsu.edu

F. Bake
German Aerospace Center (DLR), Germany
E-mail: friedrich.bake@dlr.de

L. S. Hultgren
National Aeronautics and Space Administration (NASA), USA
E-mail: Lennart.S.Hultgren@nasa.gov

T. Poinsot
Institute de Mecanique des Fluides de Toulouse, France
E-mail: poinsot@cerfacs.fr

Introduction

Core noise is projected to be an important component of propulsive noise of the next generation aircraft (see Ref. [1]). This is because traditionally dominant noise components such as jet noise and fan noise have been substantially reduced in recent years by the introduction of high bypass ratio engines, by the use of geared fans and by incorporating innovative fan blade designs including sweep and lean technology and the use of advanced acoustics liners and other noise suppressors. Another significant reason is that there is a strong push for green engines. Green engines are designed for high efficiency and low emission. To achieve these goals, these engines are to operate at a much higher temperature and at the fuel-lean limit. These changes, invariably, will make the combustion processes highly unsteady resulting in an increased emission of direct combustion noise and hot spots. When hot spots from the combustor are convected past a turbine or a flow constriction such as a nozzle in the flow path of the engine, sound will also be generated, Ref. [2–4]. This is referred to as indirect combustion noise. Thus, a green engine could potentially produce high levels of both direct and indirect combustion noise.

Over the years, there have been a number of comprehensive reviews on combustion noise. Among them are the works of Mahan and Karchmer [5], Candel et al. [6], Duran et al. [7], Dowling and Mahmoudi [8], and Ihme [9]. The last review article by Ihme was published only last year. For this reason, we will include references from the extensive lists provided in these articles only when relevant to our discussion.

Lately, because of renewed interest in the subject, there has been a surge of publications in combustion noise (both direct and indirect). We will emphasize on the new work, especially on modeling and prediction, observed characteristics of combustion noise, and the physics and mechanisms of noise generation.

This review is divided into three parts. Part 1 is on direct combustion noise. Part 2 is on indirect combustion noise. Part 3 is on high-fidelity simulation of combustion noise. The reason behind these subdivisions is that the basic noise generation mechanisms for direct and indirect combustion noise are quite different; although both are products of combustion. It is believed that by separating the two noise components would bring clarity and put each part of the review into focus. Furthermore, high-fidelity simulation of direct and indirect combustion noise, either separately or simultaneously, will play an increasingly important role in future research and deserves a separate discussion.

Part 1. Combustion Noise (Direct)

1.1 Introduction

Direct combustion noise is generated when fuel is burnt. This suggests that to understand combustion noise, perhaps, we should first understand the processes of combustion. But this is beyond the scope of this review. In addition, it is not clear we fully understand all the intricate details of the chemical processes in the combustion of hydrocarbon fuel at this time.

We recognize that there is still a lack of fundamental understanding on how direct combustion noise is generated. Most investigators believe, with good reasons, that it has to do with heat release during chemical reaction in the combustion process (e.g. Price et al. [10], Hurle et al. [11], and Shivashankara et al. [12]). But it appears that no one has a mechanistic explanation of how sound is generated because of the heat release. Presumably, sound is generated at the flame front. But the details are blurred.

It is well known that combustion, generally, enhances turbulence. Should we include turbulence generated sound as combustion noise? How significant is this noise component as compared to the noise associated with chemical reaction? These are difficult questions that do not seem to have straightforward answers.

Combustion involves kinetic interaction at the molecular level. So it is possible that some of the characteristics of combustion noise are controlled at the molecular level. For most of us, we implicitly

assume that the dominant characteristics of combustion noise are formed at the continuum level and can be predicted using continuum equations. We are not sure if this assumption is correct.

In the literature, there are a number of illuminating theoretical and experimental works on combustion noise, Bragg [13], Smith and Kilham [14], Price et al. [10], Hurle et al. [11], Thomas and Williams [15], Abugov and Obrezkov [16], Clavin and Siggia [17], Rajaram and Lieuwen [18], and Hirsh et al. [19], just to name a few. But one of the main difficulties is that kinetic time scales and continuum time scale are widely disparate. Moreover, hydrocarbon fuel with complex molecules leads to multi-steps reactions. This makes any analytical calculation and even fully numerical computation too involved to be feasible at this time. In addition, in turbulent combustion, the effect of turbulence on the transport of fuel and oxidizer is not so easy to quantify. Because of all these reasons, there is no relatively well-developed theory.

To avoid many of the difficulties mentioned above in the development of a theory of combustion noise, Strahle [20, 21] was the first to employ Lighthill's Acoustic-Analogy method to identify the combustion-noise source term by recasting the governing equations in a certain form. Since Strahle's early work, this approach has gained a good deal of popularity. The Acoustic-Analogy formulation was originally developed by Lighthill [22, 23] in the early 1950s for the identification of the sources of jet noise and as a framework to describe its propagation to the far field. For turbulence-generated jet noise, Lighthill [22, 23] showed that the source in the Acoustic-Analogy theory is a quadropole. He also established his celebrated U^8 velocity-scaling law for jet noise by means of this method. However, during the intervening years between then and now, high quality narrow band, hot and cold jet noise data at different Mach numbers became available. As a result, more and more discrepancies between the jet-noise quadrupole theory and experimental measurements became known. About a decade ago, based on extensive experimental data, Tam et al. [24] proposed a two-source jet-noise model to replace the quadrupole representation. They showed, using single far-field microphone data, two far-field microphone cross-correlation data and jet-turbulence far-field microphone correlation data, that high-speed jet noise actually consists of two components. These two noise components are generated by the fine scale turbulence and the large turbulence structures of the jet flow. They also provided far-field data that were at variance with Lighthill's velocity-scaling law. Their data show clearly that the velocity exponent is not eight. It depends on the direction of radiation and the jet temperature. For a temperature ratio 2.7 jet, the velocity exponent is around 6.5 to 7.5 in the sideline direction and around 9 for inlet angles larger than 130 degrees.

Another problem with the Acoustic-Analogy approach is that there are several possible implementations. In the combustion-noise investigation of Bailly et al. [25], the Lighthill's [22, 23], the Phillips' [26] and the Lilley's [27, 28] formulations were invoked, with each approach yielding a different form of the combustion-noise source term. So we have three different descriptions of the noise source. This situation is rather perplexing and puzzling. It is unlike many other physical problems for which the sources are well defined. All these cause us to be unsure whether Acoustic Analogy is an appropriate way to determine the sources of combustion noise.

In view of the many uncertainties in combustion-noise theories, we believe it will be more beneficial to confine Part 1 of this article to review only experiments and empirical and semi-empirical studies devoted to modeling and prediction of combustion noise.

1.2 Basic and Simple Engine Noise Experiments

Fuel-rich combustion is uneconomical and, therefore, impractical. For this reason, we will consider only fuel-lean combustion noise. Also, since most engines use hydrocarbon fuel, we will restrict our review to hydrocarbon fuel only. However, both liquid and gaseous fuels are included.

1.2.1 Combustion Noise from Open Flames

Open flames are the simplest source of combustion noise. It has been widely studied in the past e.g. Refs. [5, 18, 29–40] and others. Interests in the noise field from an open flame or an engine are generally confined to two quantities, namely, the directivity and the spectra. It is known for a long time that the noise from open flames is nearly isotropic e.g. Refs. [41–43]. Thus most studies on combustion noise from open flames concentrated on the noise spectrum. Intensity is important but it can be computed by integrating the spectrum. Variations of the noise spectrum with burner diameter, turbulence level, flame temperature are reported in Refs. [5, 18, 29–40]. Kilham and Kirmani [33], Putnam [44], and Rajaram and Lieuwen [18] concentrated their research effort on the effect of turbulence on premixed flame noise. They used a grid to produce flow turbulence. They found that higher turbulence levels in flames give rise to higher combustion noise intensity but no effect on spectral shape. In the studies of Kotake and Takamoto [29, 34], they produced data to show that the shape of the noise spectrum and frequency at the peak of the spectrum appeared not to be dependent on burner size and shape and nor on the equivalence ratio of the fuel. In a series of papers on the results of their experimental investigations on noise from open flames, Lieuwen and Rajaram [18, 39, 40], based on their own data, reported that the spectral shape of combustion noise is independent of burner diameter, fuel equivalence ratio, flow velocity and turbulence level. Fig. 1.1 shows a collapse of several of their noise spectra into a single spectrum when normalized by the peak sound-pressure-level (SPL) and equivalent frequency. An excellent summary of the various studies of combustion noise from open flames is provided in the recent work of Rajaram and Lieuwen [45].

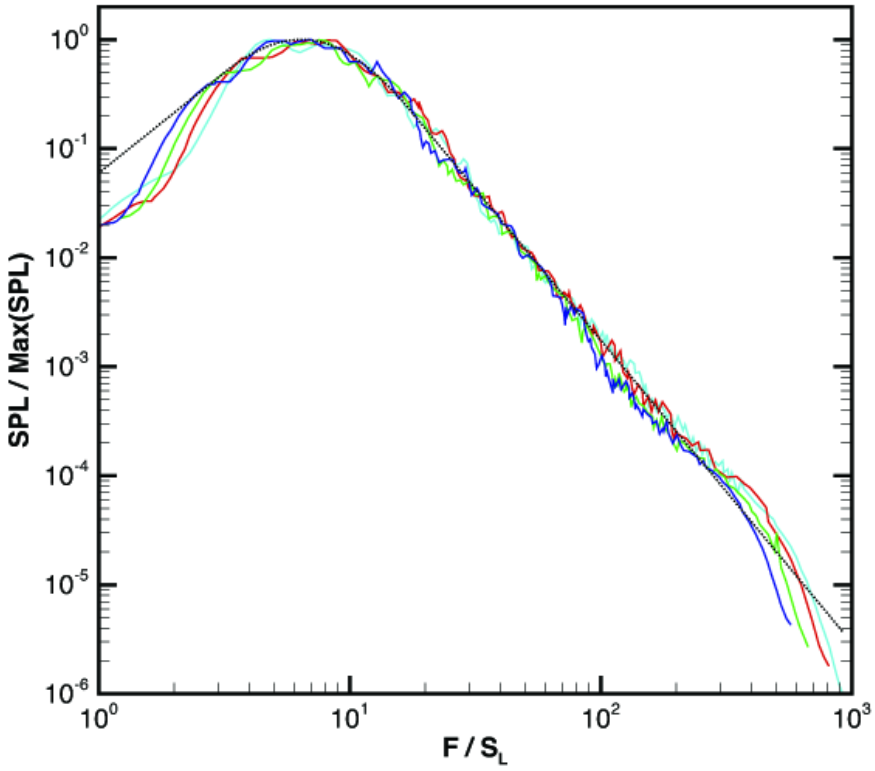

Fig. 1.1 The spectral shape of combustion noise from open flames measured by Rajaram et al. [30]. Spectra are normalized by peak SPL and equivalent frequency. Black dotted curve is the similarity spectrum, Ref. [24].

A major difficulty in studying combustion noise from open flames is that the phenomenon involves many variables/parameters. They include parameters of the flame holder geometry, the fluid flow parameters such as inflow velocity, fuel and oxidizer densities, their temperatures and turbulence level, the chemical parameters of equivalence ratio and whether the fuel is gaseous or liquid, premixed or not. With so many parameters, it is not a simple task to correlate them with the emitted noise to form simple relations experimentally.

1.2.2 Combustion Noise from Simple Engines

Large turbofan engines, invariably, have many noise sources. Many of them have intensities higher than combustion noise. Combustion noise is more likely to be observed in the measurements using smaller turboshaft engines.

Auxiliary power units (APU) are small turboshaft engines used to provide power to commercial aircraft when parked on a ramp before the main engine is turned on. Their jet exhaust velocity is around Mach 0.1 or smaller. So jet noise is exceedingly low. The dominant noise components of APUs are combustion noise and turbine noise. Turbine noise is primarily tones. So, they can readily be identified and separated out. The dominant broadband noise is combustion noise.

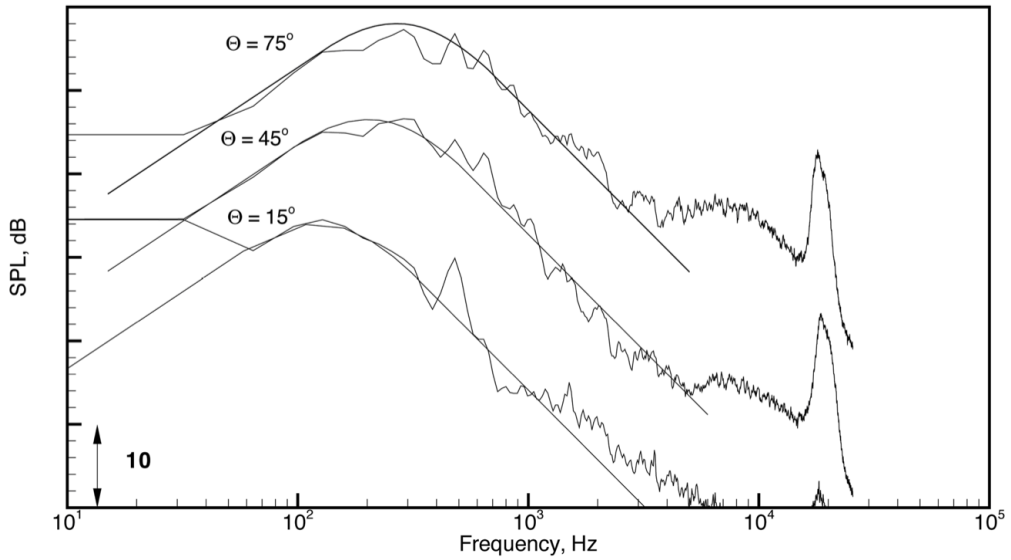

Fig. 1.2 Noise spectra of Honeywell APU RE220 at full power at three angles. Spectra displaced vertically by 10 dB for clarity. Smooth curves are the similarity spectrum, Ref. [24].

Over the years, Honeywell Aerospace Company has measured extensively the noise of their large, medium and small size APUs at high, medium and low power settings, Tam et al. [46]. In the Honeywell APU experiments, the direction of jet exhaust from the tail pipe is the zero degree angle. The directivity covers the angular sectors of $\pm 85^\circ$. The data set has accumulated to more than 100 spectra. All measured spectra show a dominant broad peak as shown in Fig. 1.2. There are some minor peaks superimposed on the main spectrum. These peaks are known to be tail-pipe resonances. Tam et al. [46] after examining the entire data set found that all the spectra had the same spectral shape regardless of the size of engine, power setting and direction of radiation. The spectral shape they found was identical to the large turbulence structures similarity spectrum of high-speed jet noise, Ref. [47]. The similarity spectrum is shown as the smooth spectrum in Figs. 1.1 and 1.2.

Fuel efficiency for APU is nearly 99%. On assuming that the acoustic pressure fluctuations produced by combustion are proportional to the heat release rate, the following formula relating the noise intensity, I, and the fuel consumption rate, $\dot{m}_f$, can easily be derived,

$$I \propto \dot{m}_f^2 / r^2 , \tag{1}$$

where r is the distance to the observer. The proportionality constant depends on the engine size and design. This simple formula was validated by means of the Honeywell data, Ref. [46]. That this is true, in turn, confirms the proposition that noise intensity generated by combustion is proportional to the rate of heat release.

In the open literature, engine combustion noise other than those of APUs is rarely reported. Most engine companies treat their noise data as proprietary. There is no question that the proprietary issue has hampered the advances of the science of combustion noise and the development of prediction model and formulas.

1.2.3 The Shape of Combustion Noise Spectrum

Because the phenomenon of combustion involves many variables and processes, theoretical advances in understanding and predicting combustion noise are difficult. Historically, for physical problems of such complexity an empirical approach often becomes a good first step. Since the 1950s, significant progress has been made by many investigators in their studies of combustion noise from open flames and small turboshaft engines. However, combustion-noise experiments are not easy to perform and the range of variables that may be included in the tests is limited. Nevertheless, one common finding reported in the literature is that the spectral shape of combustion noise is relatively insensitive to changes in experimental variables. Tam [48] examined the largest, to date, set of existing observations and proposed that the combustion-noise spectrum is truly universal and is described by the similarity noise spectrum of the large turbulence structures of jet flows (see Figs. 1.1 and 1.2). He supported the proposition by showing good comparisons between the similarity spectrum and numerous combustion noise spectra from open flames, non-premixed flames at low Mach number, can-type combustors, APUs and turbofan engines at low power. A universal spectral shape, upon verification by further experimentation, would be very useful for identification of combustion noise in environments where there are more than one noise source and for providing a validation test for potential combustion-noise theories.

1.3 Modeling and Prediction

Efficient low-order noise modeling and prediction techniques are essential for system-level community-noise projections and engineering trades at the preliminary/conceptual design stages of aircraft-propulsion systems. In general, the semi-empirical methods for turbofan core/combustion-noise prediction in use today have their roots in developments that mainly took place during the 1970s. These early advances in core/combustion-noise modeling are discussed in the review chapter by Mahan and Karchmer [5], and references therein. The approaches used can broadly be divided into fundamental and applied research avenues.

From a fundamental-research perspective, it was commonly postulated that the noise generated in an aircraft combustor is closely related to that of an open flame. Theories and models for open-flame noise were developed and validated by correlating observations with variations in physical parameters. Successively more complex situations were then considered such as the effects of ducting on flame noise and finally combustor-rig experiments. References and a further discussion can be found in the comprehensive review article by Strahle [49] and in Hultgren et al. [50]. It was found that the radiated sound from

an open turbulent flame has a relatively universal spectrum. On an 1/3-octave basis, it gradually rises to a peak somewhere in the 300 to 600 Hz frequency range and monotonically falls off thereafter.

In principle, to model the direct combustion noise emanating from an aircraft engine, an understanding is needed of the acoustic pressure field inside a combustor, how it is affected by changes in engine-operational parameters, and finally its further propagation and interaction with turbine stages through the engine-internal flow path. Inside actual combustors, operating either in rigs or engines, the confined geometry leads to the existence of a multitude of acoustic modes, (m,n), where m and n denote the azimuthal and radial mode numbers, respectively. These modes are driven by the unsteady heat release of the combustion and their amplitudes are generally statistically independent. However, for the common situation where there is no significant global swirl present in the combustor, then modes with opposite azimuthal mode numbers, but identical radial mode numbers, can be taken to be of the same random amplitude. The plane wave mode $(0,0)$ can always propagate, but the other modes can only propagate if the frequency is higher than a mode-dependent cut-off/cut-on value. If the frequency is less than this value, the mode is evanescent.

Karchmer [51] and, more recently, Royalty and Schuster [52] have documented the modal structure of the unsteady pressure field in aircraft-engine non-premixed combustors. The former [51] utilized a ducted full-scale YF102 annular-combustor in a rig experiment, whereas the latter [52] analyzed measurements obtained in an actual TECH977 research turbofan engine. These investigations both showed that the acoustic pressure spectrum at the exit of a real combustor has a multi-peak nature/structure and that individual modes could be uniquely identified within separate frequency bands. The plane-wave $(0,0)$ mode dominates for the lowest frequencies up to the cut-on frequency of the $(\pm 1,0)$ mode pair. For higher frequencies, the most recently cut-on mode, or mode pair, dominates the unsteady pressure field; that is, successively higher azimuthal modes dominate with increasing frequency. Radial modes, $n \neq 0$, in general, do not appear to play a role due to their cut-off/on frequency values being higher than the direct-combustion-noise frequency range. Similar results were obtained by Krejsa and Karchmer [53] for the core-nozzle unsteady pressure field of an AiResearch QCGAT turbojet engine. They found that the plane-wave $(0,0)$ mode was dominant up to about 800–900 Hz at the tail-pipe exit.

Karchmer [51] concluded that the basic source generating mechanism itself has a relatively smooth and featureless spectral shape, but the geometry of the combustor is extremely effective in promoting resonant modes and thus modifying the unsteady pressure spectrum in the combustor. This conclusion was echoed by Schuster and Lieber [54], who also suggested that the far-field spectrum can be thought of as the product of a single-peak broadband combustion noise spectrum, that is related to the spectrum of an open turbulent flame, and a spectral transfer function that represents the resonance and propagation effects in the engine core and exhaust. They [54] observed that "it is unrealistic to expect that a single transfer relation will be generally applicable to the wide variety of combustor, turbine and exhaust geometries." However, as pointed out by Mahan and Karchmer [5], the higher modes are often cut-off in the smaller diameter turbine and core nozzle and are thus unable to propagate efficiently through the engine to the surroundings. As a consequence, it is generally accepted that the direct combustion noise emanating from turbofan engines is dominated by the plane-wave mode and therefore effectively has a single-peak spectrum. That is, spectral peaks associated with the non-plane-wave modes are in practice reduced to such an extent that their amplitudes are well below the dominant plane-wave peak as well as the levels of other propulsion-noise components. For current generation engines, jet noise in particular dominates even the peak value of the direct combustion noise except at low engine-power settings. The situation can be different for auxiliary power units (APUs) due to their low exit velocities and often long tailpipes, however. The low exit velocities significantly reduce the importance of jet noise and makes combustion noise the dominant low-frequency exhaust noise source for APUs. Schuster and Lieber [54] also found that APU far-field combustor-noise peak frequencies correlated strongly with the exhaust duct length and mean exhaust duct sound speed according to plane-wave radiation from an unflanged circular pipe.

A substantial amount of applied research, relating measured real-engine noise levels to operating parameters, was published in the open literature during the 1970s. This work, eg. [55–59], was mainly carried out by aircraft-engine company researchers in the United States, often with support from the Department of Transportation/Federal Aviation Administration (DOT/FAA) or the National Aeronautics and Space Administration (NASA). Largely informed by the physical understanding obtained from the early fundamental studies briefly described above, the General Electric Company (GE) [59] and Pratt & Whitney (PW) [58] determined semi-empirical, engine-manufacturer-specific formulas for the total radiated acoustic power, with model coefficients/constants determined using rig testing of isolated components and full-engine static-test data. These models [58, 59] also included simple frequency-independent formulas to account for the turbine attenuation of the broadband noise originating in the combustor. The decoupled far-field directivity and spectral distribution were obtained empirically from full-engine static tests.

In general, each of these acoustic-power prediction tools [58, 59] showed good agreement with data from the engine manufacturer that developed the method, but not necessarily with data from other companies [5, 60]. Zuckermann [60] suggested that the need for distinct models may be caused by differences in burner design philosophy. A common difficulty encountered during the development of these methods was that the measured total far-field acoustic signature in static-engine tests normally had to be adjusted by subtracting the low-frequency jet noise using an appropriate model to reveal the core noise. This is because, in the absence of forward-flight effects, combustor noise is not a dominant noise source even at low engine-power settings. This makes the quality of the results somewhat dependent on the accuracy, particularly at low frequencies, of the jet-noise model used.

In 1980, The Society of Automotive Engineers International (SAE) adopted the method developed by GE [59] as the SAE ARP876 [61] technical standard for the prediction of noise from conventional combustors installed in gas-turbine engines. This semi-empirical direct-combustion-noise model [59, 61] still forms the kernel of the core-noise module in the NASA Aircraft Noise Prediction Program (ANOPP) [62, 63] and it is referred to therein as the SAE method. The NASA-ANOPP core-noise module also contains several extensions to the GE/SAE formulation. The GE/SAE, the PW, and the NASA-ANOPP methods are further discussed in subsections below. Tam [48] provides a further discussion of the spectral distributions used in the methods as well as a suggestion for an improved universal far-field spectrum for direct combustion noise. See the discussion in Section 1.2.3 above.

1.3.1 A Common Form of the Semi-Empirical Models

A common feature of most of the semi-empirical models for direct combustion noise is that the far-field directivity and spectral distribution are decoupled. In this case, the (dimensional) combustion-noise mean-square pressure in each 1/3-octave band (b), in the absence of atmospheric attenuation, is given by

$$< p'^2 >^{(b)} = \frac{\rho_\infty c_\infty \Pi D(\theta) S(f_b)}{4\pi r_s^2} \tag{2}$$

for a static-engine test, where r_s is the distance between the source and the observer and ρ_∞ and c_∞ are the ambient density and speed of sound at the observer location. Π is the total radiated acoustic power by the source. $D(\theta)$ is a directivity function that depends only on the polar angle θ and satisfies the normalization condition

$$\int_0^\pi D(\theta) \sin\theta \mathrm{d}\theta = 2\,. \tag{3}$$

$S(f_b)$ is a spectrum function satisfying

$$\sum_b S(f_b) = 1 \tag{4}$$

and f_b is the 1/3-octave-band center frequency. Note that the total radiated acoustic power at the distance r_s from the source

$$\int_A \frac{\sum_b < p'^2 >^{(b)}}{\rho c} \mathrm{d}A = \Pi \,, \tag{5}$$

where $\mathrm{d}A = r_s^2 \sin\theta \mathrm{d}\theta \mathrm{d}\phi$, with ϕ denoting the azimuthal angle. That is, in the absence of atmospheric attenuation, the total radiated acoustic power Π is preserved as the acoustic waves propagate towards the observer.

The sound pressure level $SPL^{(b)}$ in an 1/3-octave frequency band, the overall sound pressure level $OASPL$, and the overall power level $OAPWL$ are given by

$$SPL^{(b)} = 10\log_{10}(< p'^2 >^{(b)} / p_{ref}^2) \,, \tag{6}$$

$$OASPL = 10\log_{10}(\textstyle\sum_b < p'^2 >^{(b)} / p_{ref}^2) = 10\log_{10}[\rho_\infty c_\infty \Pi D(\theta)/4\pi r_s^2 p_{ref}^2] \,, \tag{7}$$

$$OAPWL = 10\log_{10}(\Pi/\Pi_{ref}) \,, \tag{8}$$

where $p_{ref} = 2 \times 10^{-5}$ Pa and $\Pi_{ref} = 1 \times 10^{-12}$ W if SI units are used. Note that some authors use PWL to denote the overall power level and also simply refer to it as the power level. Guided by [61], here

$$PWL^{(b)} = OAPWL + 10\log_{10} S(f_b) \tag{9}$$

denotes the acoustic power radiated in all directions associated with a given 1/3-octave frequency band (b), however, and is referred to as the power-level spectrum.

1.3.2 The GE/SAE Model

In the GE/SAE direct-combustion-noise model [59, 61], the total radiated acoustic power is given by

$$\Pi = 10^{K/10} c_o^2 \dot{m}_c \left(\frac{T_{t,ce} - T_{t,ci}}{T_{t,ci}}\right)^2 \left(\frac{P_{t,ci}}{P_o}\right)^2 \times F_{TA} \,, \tag{10}$$

where F_{TA} is a turbine attenuation, or loss, factor and is given by [56, 61]

$$F_{TA} = F_{TA,GE} = \left(\frac{\Delta T_{des}}{T_o}\right)^{-4} . \tag{11}$$

The constant $K = K_{SAE} = -60.53\ldots$ [61]. $\dot{m}_c$ is the mass flow rate into the combustor, $T_{t,ci}$ and $T_{t,ce}$ are the total temperature at the combustor inlet and exit, $P_{t,ci}$ is the total combustor-inlet pressure, and P_o and T_o are the reference (static) pressure and temperature. The reference state, denoted by the subscript 'o', is the standard sea-level conditions ($P_o = 101.325$ kPa, $T_o = 288.15$ K, $c_o = 340.294$ m/s, in SI units). ΔT_{des} is the design-point temperature drop across the turbine. If this is not known, the temperature drop at takeoff can be used. Note that the acoustic transmission loss is independent of both the frequency and the engine operating condition. The spectrum and directivity functions are defined in SAE ARP876 [61]. In particular, the spectrum is the SAE single-peak in-flight jet-noise spectrum with the peak frequency fixed at 400 Hz. Equation (10), with $K = K_{SAE}$, combined with (11) for the turbine-transmission loss, will be referred to as the SAE formulation herein. The SAE ARP876 standard [61, Appendix D] also contains a background history of its development as well as an extensive list of relevant references.

1.3.3 The Pratt & Whitney Model

Also during the latter half of the 1970's, researchers at Pratt & Whitney [57, 58] developed a semi-empirical prediction method for direct combustor noise. They derived models for the total acoustic power level, turbine coupling/ transmission losses, and peak frequency; and they empirically determined model constants, the directivity pattern, and a universal normalized spectral distribution using a range of burner-rig and full-scale static engine tests.

In this model, the total radiated acoustic power is given by [5, 58]

$$OAPWL = 10\log_{10}\left[\frac{1}{N_f}A_c^2 P_{t,ci}^2\left(\frac{\dot{m}_c\sqrt{T_{t,ci}}}{P_{t,ci}A_c}\right)^4\left(1+\frac{h_{PR}F_{st}}{c_p T_{t,ci}}\right)^2 F_c^2\right] + 132 + 10\log_{10}(F_{TA}), \tag{12}$$

where N_f is the number of fuel nozzles in the combustor, A_c is the combustor cross-sectional area, h_{PR} is the constant-pressure fuel heating value, c_p is the specific heat at constant pressure, F_c and F_{st} are the combustor fuel-air ratio and the stoichiometric fuel-air ratio; and as earlier $\dot{m}_c$, $P_{t,ci}$, and $T_{t,ci}$ are the mass flow rate and total pressure and temperature at the combustor inlet. The frequency-independent, turbine-attenuation factor is given by

$$F_{TA} = F_{TA,PW} = \frac{4\zeta(\ell/\pi D)}{(1+\zeta)^2} = \frac{0.8\zeta}{(1+\zeta)^2}, \tag{13}$$

where $\zeta = \rho_{te}c_{te}/\rho_{ti}c_{ti} \approx (P_{t,te}/P_{t,ti})\sqrt{T_{t,ti}/T_{t,te}}$, with the subscripts '$te$' and '$ti$' indicating turbine exit and inlet, is the ratio of the characteristic impedances across the turbine. ℓ is the circumferential correlation length of the direct-combustion noise at the combustor-turbine interface, D is the outer diameter of this interface. Mathews and Rekos [58] found that combustor-rig and transmission-loss-corrected engine data agreed when $\ell\pi/D = 0.2$, which led to the final, and simplified, result in (13). Note that the acoustic transmission loss depends on the engine operating condition in the PW formulation.

Unfortunately, the argument of the base-ten logarithm, i.e., the quantity inside the square brackets, in (12) is not dimensionally correct. It should be nondimensional, but it is not! This means that the constant (= 132, here) depends on the choice of units for the independent variables. Consequently, to use this formula (12), customary US engineering units must be used in the input, see [58] for unit details.

The peak frequency involves burner design and geometry parameters and is given by

$$f_p = K_f\frac{Rh_{PR}}{c_p}\left(\frac{\dot{m}_f}{P_{t,ci}}\right)_{des}\frac{1}{A_c L_c}, \tag{14}$$

where R is the gas constant, $\dot{m}_f$ is the fuel mass flow rate, L_c is the combustor length, and the subscript 'des' indicates evaluation at the design point (which can be taken as takeoff conditions).

1.3.4 The NASA-ANOPP Combustion-Noise Models

The purpose of the NASA-developed modular computer program ANOPP is "to predict aircraft noise with the best currently available methods" [64]. In order to maintain and enhance the program, NASA has continued to contract with industry to evaluate ANOPP against fly-over and real-engine data and to suggest improvements to its modules. These investments have over the years led to significant improvements in the capability of ANOPP.

The GE/SAE direct-combustion-noise model [59, 61] was the first method implemented in the ANOPP [62, 63] core-noise module GECOR and is referred to as the SAE option therein. However, in contrast to the original SAE formulation, the reference state, denoted by the subscript 'o' in (10) and (11), is in

ANOPP taken to be the actual ambient conditions, which generally are different from standard sea-level values. Equations (10) and (11), with $K = K_{SAE}$ and relaxed reference state, will be referred to as the ANOPP-SAE-GE formulation herein.

The ANOPP prediction capability was extended to a larger class of engines during the mid 1990s by updating the propulsion-noise modules in ANOPP to also cover small turbofan engines such as typically used by smaller regional-transport and business aircraft. For the GECOR module, this led to the introduction of a new small-engine (SmE) option. The SmE-option formulas are identical to those of the SAE option, except that the acoustic power level is reduced by 4 dB, i.e., the constant $K = K_{SmE} = -64.53\ldots$ in (10). Equation (10), with $K = K_{SmE}$, combined with (11) for the turbine-transmission loss, will be referred to as the ANOPP-SmE-GE formulation herein.

Hultgren [65] used time-series data, obtained during the NASA/Honeywell Engine Validation of Noise and Emission Reduction Technology program [66] (EVNERT), to assess the turbine transfer of direct combustion-noise and to develop an update to the turbine-attenuation formula used in ANOPP. The program used the Honeywell TECH977 research turbofan engine, which is typical of a business-jet application in the 31–36 kN (7,000–8,000 lbf) thrust class. The true combustion-noise turbine-transfer function was educed from the EVNERT data by applying a three-signal technique utilizing one sensor in the combustor and two at the turbine exit. Note that the true turbine gain factor is always underpredicted (i.e., attenuation is overestimated) by a directly measured one, using only two sensors, because of a positive bias error caused by the presence of pressure fluctuations in the combustor that are uncorrelated with the propagated direct-combustion noise [65]. The resulting gain factors (< 1) were compared with the corresponding constant values obtained from the GE and the simplified PW acoustic-turbine-loss formulas, (11) and (13). Hultgren [65][1] found that the gain factor obtained from the simplified PW formula (13) agreed better with the experimental results for frequencies of practical importance. He also found that replacing the GE combustor-noise turbine-attenuation function (11) in Hultgren and Miles [67] with the simplified PW one (13) clearly improved the total-noise predictions and also improved the combustion-noise predictions. The latter comparison was not as conclusive as the former due to the inherent difficulty in extracting the combustion-noise component from the total noise signature over its whole frequency range. However, the former would not be true if the combustion-noise component predictions had not been improved by the attenuation-formula change.

The ANOPP core-noise module was subsequently updated to allow the user a choice of using either the GE or PW turbine transmission formulas for both the SAE and SmE options, i.e., the two additional configurations ANOPP-SAE-PW and ANOPP-SmE-PW were added. The current ANOPP module also contains a separate intermediate-narrow-band method [54] to account for tail-pipe resonances.

1.3.5 European Semi-Empirical Models for Aircraft-Noise Prediction

Since the early 2000s (in particular the last ten years), there has been an upswing in European aircraft-noise research and prediction-tool development. Historically, most of the development of non-proprietary models and semi-empirical tools for the prediction of aircraft noise took place in the US, but this is now changing. Several efforts are underway (or at a mature stage), some of which are of the database type, using flyover data from existing aircraft, and some of which are for physics-based semi-empirical models. Some of the latter efforts are briefly discussed below. Even though these efforts are very impressive and overall advance the state-of-the-art, it appears that any advancement of semi-empirical models for direct-combustion noise has yet to take place.

ANOTEC Consulting SOPRANO Tool. Based on the description found in Ref. [68], the SOPRANO tool for aircraft-noise calculations, developed by ANOTEC Consulting during the European SILENCE(R)

[1] Due to a typographical error, the formula in [65] corresponding to Eq. (13) is inverted, but the computations therein are correct.

research program, contains several airframe- and propulsion-noise (including core) components implemented from models available in the open literature at that time. The core noise is predicted using the SAE ARP876 method.[2] Since then SOPRANO has been extended with additional modules mainly within various European research and development projects, but no other core-noise module has been included.[2]

DLR PANAM Prediction Tool. The German Aerospace Center (DLR) developed the Parametric Aircraft Noise Analysis Module (PANAM) overall-aircraft-noise prediction tool [68–70] to enable comparative design studies with respect to airport-community noise and to identify promising low-noise technologies at early aircraft-design stages. Each included airframe and propulsion noise-source is simulated using a semi-empirical model. The engine-noise models are based on existing models in the literature. However, it appears [69, 70] that only the two dominant propulsion-noise sources for current generation aircraft, namely jet and fan sources, are currently implemented in the engine-noise module.

ONERA IESTA Project. The French Aerospace Lab ONERA (Office National d'Etudes et de Recherches Aérospatiales) developed a generic simulation platform, IESTA (Infrastructure for Evaluating Air Transport Systems), for the purpose of assessing future air-transport concepts [71]. The prediction of aircraft noise is a significant part of determining the environmental impact (noise and emissions) of these concepts. This capability has been implemented in an acoustic model labeled CARMEN [72], which consists of three modules: CEASAR-S containing acoustic-source models, CEASAR-I modeling installation effects (reflections and scattering by aircraft surfaces, etc.), and SIMOUN propagating the sound field to observers on the ground. The CARMEN methodology is similar to the ones used by NASA ANOPP [62, 63] and DLR PANAM [72]. It is not clear from the open literature, if a core/combustion-noise model has been implemented in CEASAR-S, at least it appears not normally used in predictions. It is often stated that CEASAR-S "computes noise source levels coming from main noise components of current jet aircraft: jet, fan, high-lift devices and landing gear" [73], see also [72].

1.3.6 Other Codes

All major engine and airframe companies have proprietary in-house noise-prediction codes with capabilities similar to those of ANOPP. Their confidential, semi-empirical, direct-combustion-noise prediction methods are most likely based on the models described herein. Because each company has a large database of test results (including noise-certification tests), their models can be tailored for the engine type (for an open example of this see [74]), and maybe even specific aircraft, under consideration.

The companies more than likely also have multiblade-row actuator-disk-type codes (eg.[8, 74, 75]) to determine the transfer of direct noise and the generation of indirect combustion noise by the turbine. In general, this type of code needs somewhat detailed mean-line data for each turbine stage in order to solve a matrix problem for the transmission/generation of noise. Consequently, this type of codes might not be used directly in first-cut exploratory studies, but rather later when noise estimates are refined or to tune parameters in simpler semi-empirical models.

Part 2. Entropy Noise (Indirect Combustion Noise)

2.1 Introduction

Unsteady combustion processes in the combustor of an engine produce direct combustion noise as well as entropy (hot and cold spots) and vorticity waves. These waves are convected downstream by the mean

[2] N. van Oosten, private communication, April 2017

flow. Indirect combustion noise or entropy noise is generated when the hot and cold spots are strongly accelerated past a high-pressure turbine or through the non-uniform flow in the ducting and nozzle of the engine flow path. For a long period of time, indirect combustion noise was merely a theoretical concept. Its existence lacked experimental confirmation. In the following, we will first describe the fundamental experiment that proves the existence of indirect combustion noise/entropy noise by Bake et al. [4, 76, 77, 78, 79, 80]. The experiment used a specially designed test facility. We will then review the status of our understanding on indirect combustion noise for the present generation engines. This is followed by a review on the state of art in modeling and prediction of entropy noise.

We would like to note that just as entropy noise is generated when entropy waves are convected past a highly non-uniform flow, the convection of vorticity waves past such a flow also generates noise. This was demonstrated by Kings and Bake [81] and Kings et al. [82] in a vorticity pulse experiment using a Vorticity Wave Generator test rig. Following this experiment, Kings et al. [83] repeated their investigation successfully using broadband small scale vorticity waves as input. Further validation of vorticity noise was provided by an experiment of Fischer et al. [84].

What is the mechanism responsible for the generation of entropy noise? Since the beginning of entropy noise research, the generation mechanism has, generally, been attributed to mode coupling. The idea is that a uniform flow can support three types of independent small amplitude disturbances, Chu and Kovasznay [85]. They are the entropy waves with fluctuations in temperature and density only, the vorticity waves with fluctuations in velocity only and the acoustic waves with fluctuations in all flow variables. Now, if entropy waves are convected into a non-uniform flow, the flow can no longer support entropy disturbances by themselves. The disturbances in the non-uniform flow cannot consist of temperature and density components alone. They will now have pressure and velocity components too. In other words, pure entropy blobs cannot exist in non-uniform flows. This suggests that there is coupling of the three wave modes leading to pressure fluctuations and hence noise radiation.

The idea of mode coupling is, without doubt, correct. Nevertheless, it is somewhat of an abstract concept. To explain the noise generation mechanism in more simple physical terms Tam and Parrish [86] performed a numerical experiment in which a narrow Gaussian entropy pulse is sent through a convergent-divergent (C-D) nozzle. The reason for using a single narrow pulse is that in such an experiment there will only be one possible noise source. Therefore, there is no room for ambiguity as to where and how the sound is generated. Figure 2.1 shows the distribution of pressure and density fluctuations in a subsonic C-D nozzle at six different instances as the entropy pulse makes its way through the nozzle. In each figure, the entropy pulse is represented by a dotted line, with corresponding density scale on the left border, and the generated pressure wave is represented by a solid line, with corresponding pressure scale on the right border. At station 1, the pulse is in the upstream uniform duct, so the pressure is zero everywhere, since the waves are uncoupled. At station 2, the pulse has just entered the convergent part of the nozzle, and the pressure just ahead of the pulse drops to a negative value. This causes the entropy pulse to radiate a rarefaction wave into the downstream region so as to maintain pressure balance at the pulse. At station 3, the entropy pulse approaches the nozzle throat, $x = 0$. Here, the pressure just in front of the pulse becomes more negative. So a stronger rarefaction wave is radiated ahead. At station 4, the entropy pulse has passed through the nozzle throat into the divergent part of the nozzle. The pressure just ahead of the entropy pulse is now positive. Again, to maintain pressure balance, a compression wave is radiated ahead of the pulse. There is a switch from radiating rarefaction waves to compression waves when the entropy pulse crosses the nozzle throat. At station 5, the radiated sound pressure remains positive or it is still a compression wave. Finally, at station 6, the pulse reaches the downstream uniform region of the duct. As expected, there is no more sound radiation.

Notice that the half-width of the entropy pulse expands and then contracts as the pulse is convected through the convergent and then the divergent part of the nozzle. This provides a clue on how sound is generated. Fig. 2.2 illustrates the sound generation processes in the convergent part of the nozzle. In this part of the nozzle, the mean flow velocity increases toward the throat (see the first inset below the nozzle

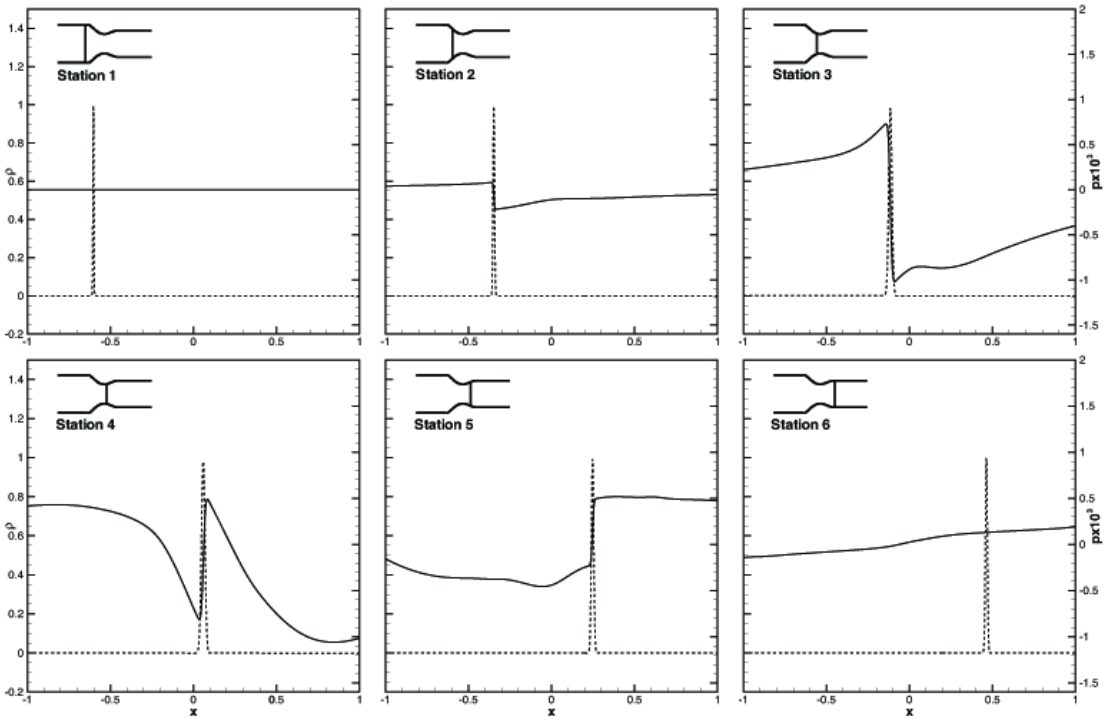

Fig. 2.1 Instantaneous density and pressure distributions inside a C-D nozzle at six instances during the passage of an entropy pulse through the nozzle. Dotted line represents density (left scale), solid line represents pressure (right scale). Nozzle throat is at $x = 0$.

in Fig. 2.2). Since the entropy wave pulse is convected downstream by the mean flow, this makes the front part of the pulse move faster than the back part of the pulse. In turn, this difference in speed causes the pulse to expand in width as indicated in the second inset of Fig. 2.2. The mass of the pulse is constant, so the density in the front part of the pulse decreases. Now, the flow is adiabatic because viscous dissipation and thermal conduction are negligible. It follows that a drop in density will lead to a drop in pressure (see the third inset of Fig. 2.2). When the pressure in the front part of the pulse decreases, pressure balance between the pulse and the gas in front requires the emission of a rarefaction wave. Once the entropy pulse crosses over to the divergent side of the nozzle, the processes are reversed. In this part of the nozzle, the width of the entropy pulse contracts because the front part of the pulse now moves slower than the back part of the pulse. As a result, the density in the front part of the pulse increases and a compression wave is emitted. This is shown in Fig. 2.1.

To provide further support for the above proposed sound generation processes, the case of a similar pulse solution but for a supersonic nozzle was also investigated. Unlike a subsonic nozzle, the mean flow velocity of a supersonic nozzle increases downstream over the entire length of the C-D nozzle. Now, it was found that the entropy pulse radiated rarefaction waves in the downstream direction throughout its entire passage through the nozzle. This is completely consistent with the sound generation mechanism proposed in Fig. 2.2 and thus confirms its validity.

2.2 Fundamental Experiments

The first experimental investigations aiming to confirm the existence of indirect combustion noise in the 1970s were conducted by Zukoski and Auerbach [87] and Bohn [88]. They used a facility made up of

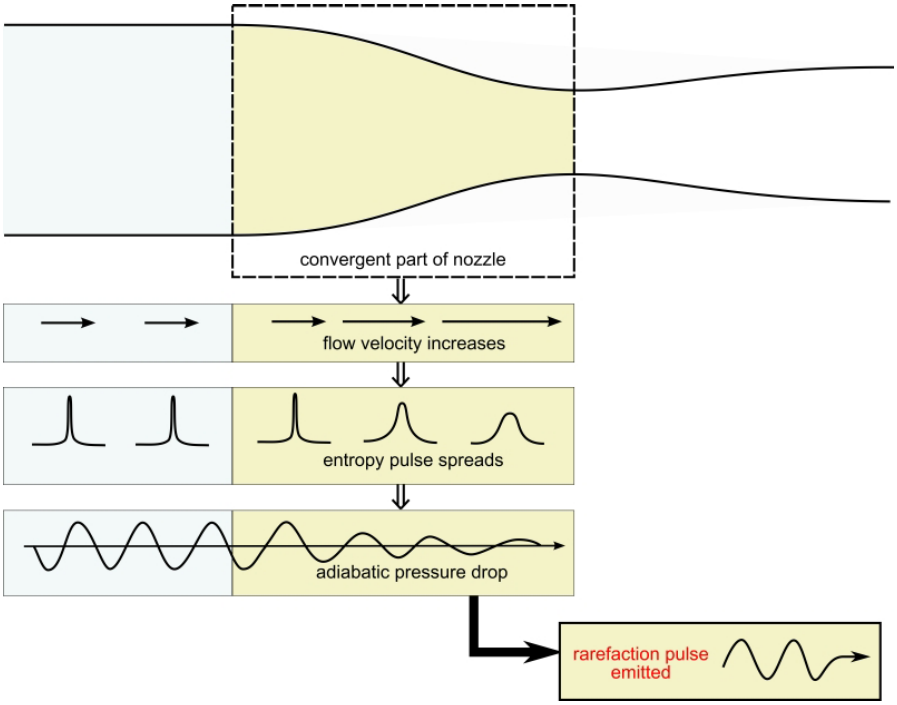

Fig. 2.2 Indirect combustion noise generation processes in the convergent part of a C-D nozzle. Flow is from left to right. Entropy pulse enters from the left end of nozzle.

a long channel connected to a nozzle. Temperature fluctuations were generated by an electric heater. Unfortunately, the amplitude of the induced temperature was very small, approximately 1 K. In addition, due to the lack of data post-processing capability at that time, clear identification of indirect combustion noise was not possible. Strahle and Muthukrishnan [89] in a combustion noise experiment attempted to correlate the measured total combustion noise power with their theory. They employed a combustor test rig with an open outlet. With an open outlet, only weak velocity gradients were able to develop inside the test facility. Because of the lack of strong velocity gradient indirect combustion noise was not observed. Muthukrishnan et al. [90] performed a coherence analysis involving different sensor signals inside and outside the combustion chamber. They reported that they were able to separate the combustion noise components of their aero-engine combustor test rig. The result showed a dominating broadband entropy noise contribution in the total noise spectrum. Similar experiment was reported by Guédel and Farrando [91] using a Turbomeca helicopter engine. They used a three-signal coherence technique for noise separation. They found a low frequency sound source located between the combustion chamber and the low-pressure turbine.

The first successful experiment proving the existence of entropy noise was carried out in 2009 by Bake et al. [92, 93]. A specially designed Entropy Wave Generator (EWG) test facility was used in their experiment. The test setup is sketched in Fig. 2.3. It consists of a tube in which entropy waves were produced by an electric heating module using thin platinum wires. Downstream of the EWG module, the flow passed through a C-D nozzle. Acoustic pressure signals were measured by wall mounted microphones in the tube section downstream of the nozzle. The test facility was designed to allow a broad parametric study including variation of the amplitude of temperature fluctuations, the C-D nozzle Mach number and the convection/propagation distance between the heating module and the C-D nozzle. When the EWG is turned on for a short period of time (e.g 10 or 100 ms), an entropy wave is generated. This pulse is convected downstream by the mean flow. If, indeed, indirect combustion noise is generated during the

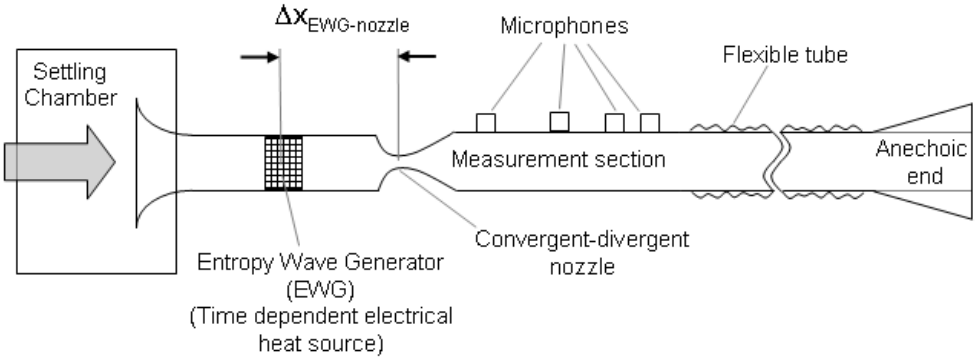

Fig. 2.3 Sketch of the Entropy Wave Generator (EWG) test facility.

passage of the entropy pulse through the nozzle, the time of arrival of the sound pulse can be measured accurately by the microphones housed in the downstream section of the nozzle. By varying systematically the distance between the heating element and the C-D nozzle, it is possible to show unambiguously that sound is produced inside the nozzle at the time when the entropy pulse is passing through the nozzle. In this way, Bake et al. [92, 93], for the first time, succeeded in providing direct and irrefutable evidence of the generation of indirect combustion noise.

Since this seminal demonstration of the generation of indirect combustion noise, there has been a deluge of publications on this subject. By using the EWG test rig results, some of these [94–98] give an enhanced model description for entropy noise—basically succeeding the theory of Marble and Candel [3]. The compactness and linearity assumption have been examined [98, 99] yelding for example improved phase predictions. Furthermore, numerical simulations have been conducted in order to assess the model capabilities [100] as well as investigating [101–103] the two-dimensional extension of the actuator-disk theory of Cumpsty and Marble [104] for turbomachinery blade rows. Other publications revealed the significance of entropy noise for combustion instability [105] even when accounting for entropy wave dispersion and dissipation effects [99]. Tam et al. [106] demonstrated the contribution of entropy noise to the noise emission of auxiliary power units (APUs). Finally Knobloch et al. [107] provided additional test cases for entropy noise generation in nozzle flows by presenting experimental results from the Hot Acoustic Test Rig (HAT).

2.3 Engine Noise Experiments

Demonstrating that indirect combustion noise can be generated in a specially designed experimental facility is important by itself. However, it is also important to show that significant amount of indirect combustion noise is actually generated in an engine. One of the difficulties in doing so is that an engine has many noise sources. So it is natural to start by trying to separate the noise components inside and outside of an engine.

Miles [108] used a coherence function technique, involving a combustor-internal pressure sensor and far-field microphones, to perform noise separation to investigate the core noise sources of a two-shaft turbofan engine. The source location technique was based on adjusting the time delay between a combustor pressure signal and a far field microphone signal by maximizing the coherence. It was discovered that the cross-spectral density band 0–200 Hz was dominated by indirect combustion noise generated by entropy waves interacting with the turbine. The signal in the 200–400 Hz frequency range was attributed mostly to direct combustion noise. Miles [109] later extended his work by using a generalized cross-correlation

function technique to study the change in propagation time to the far field of the combined direct and indirect combustion noise. In his work, a sequence of low pass filters was employed. The result showed that time delays measured in each direction is fairly consistent with one another within a range of operating conditions. He also demonstrated the feasibility of separating a mixture of direct and indirect combustion noise. The problem of noise-source separation was also investigated by Hultgren and Miles [67].

Bake et al. [110] studied the generation of entropy noise and vorticity noise by either injecting entropy or vorticity fluctuations into the flow upstream of a high pressure turbine rig. Because the flow in such a rig is highly complex, this experiment is especially challenging. In addition, more than one type of noise sources are involved. In spite of the intrinsic complexity of the problem, Bake et al. [110] were able to conclude that the dominant noise generated in the early stages of the turbine is vorticity noise. However, noise generated in the later stages of the turbine was largely entropy noise.

In the framework of the European funded TEENI project (Turboshaft Engine Exhaust Noise Identification) coordinated by Turbomeca, comprehensive acoustic measurements in and around a helicopter engine (Ardiden 1H-1 type) have been conducted, Pardowitz et al. [111]. The engine was extensively equipped with acoustic sensors not only at the combustor but also at the turbine stages and at the exhaust. Due to the fact that jet noise is low for this engine, it was anticipated that the core noise source contributions can be quantified with better accuracy than for turbofan engines. Classical coherence analysis methodologies [112–116] such as the coherent-output-power technique, the signal enhancement technique and the five-microphone method were used to study the source and propagation characteristics of the various noise components. In addition, advanced analysis methods, which combine correlation methods and mode decomposition techniques [117, 118] were applied for the first time to a real engine. The methods enabled the quantification of the different noise source contributions to the total sound power. They also yielded a detailed database for validation of numerical prediction methods. In addition, these methods allow an assessment of the contributions of the intensities of various noise sources in different frequency bands.

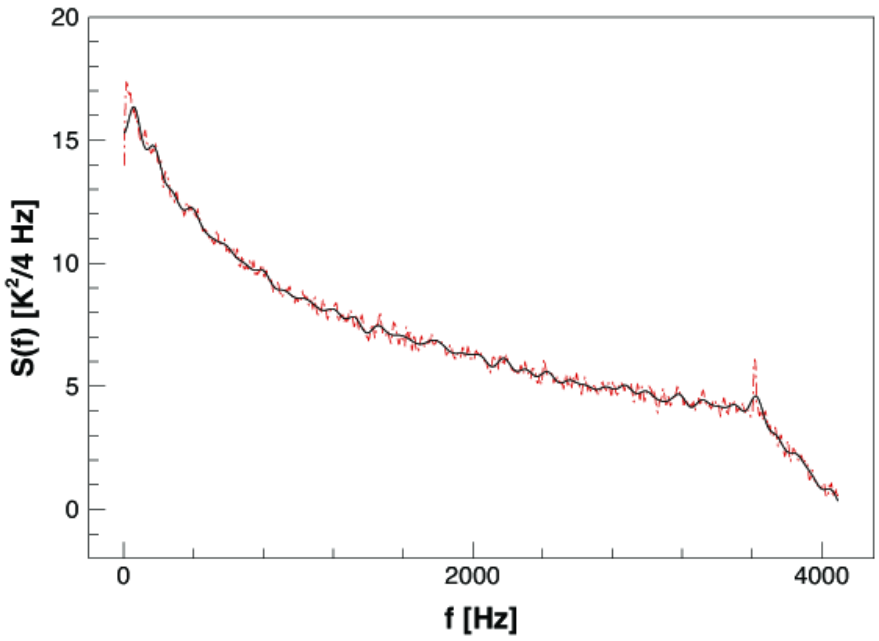

Fig. 2.4 Measured temperature fluctuation spectrum at the exit of the combustor of a Honeywell TECH977 engine, Schuster et al. [119]. Orange color line is the measured spectrum. Black color line is the stochastic model simulation spectrum (see Section 2.4).

The NASA funded study of Schuster et al. [119] concentrated on measuring several pieces of vital information relevant to indirect combustion noise generation inside an engine. Their testbed is a Honeywell TECH977 research turbofan engine. Near the exit of the combustor, the temperature is extremely high. This hostile environment makes any measurement particularly difficult. Schuster et al. [119] measured successfully the temperature and pressure fluctuation spectra at a location near the combustor exit (upstream of the high-pressure turbine), in the inter-turbine duct, and downstream of the low turbine exit. Fig. 2.4 shows their measured temperature fluctuation spectrum near the combustor exit. This is one of the first, if not the very first, of this type of measurements available in the open literature. The spectrum is dominated by relatively low frequency components. Fig. 2.5 shows a superposition of two pressure spectra. These spectra were measured using specially designed semi-infinite-tube pressure sensors, with purge flow. The black spectrum is measured at a location upstream of the high-pressure turbine. The green spectrum is measured downstream of the high-pressure turbine. The significance of Fig. 2.5 is that, by comparing the two spectra, it becomes clear that there is an increase in noise across the high-pressure turbine. The tantalizing question is 'what generates this extra noise?' There are a number of possibilities. But it is possible that it is indirect combustion noise. The challenge is how to show that it is!

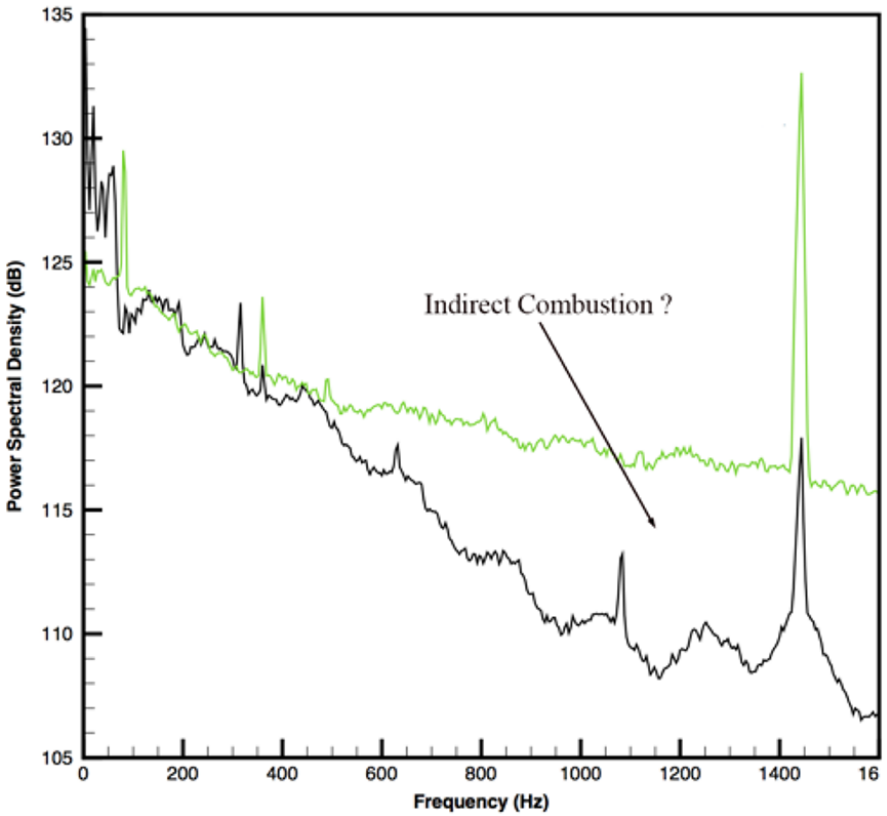

Fig. 2.5 A comparison of two pressure spectra, one measured upstream (black) and the other downstream (green) of the high pressure turbine. Origin of noise increase is unknown at this time. Data from Schuster et al. [119].

2.4 Modeling and Prediction

Prediction of indirect combustion noise began with the pioneering work of Marble and Candel [3] and Cumpsty and Marble [104, 120]. These early works have proven to be very influential. They introduced the idea of the short nozzle approximation also known as the actuator disk theory. This approximation made it possible to make quantitative prediction of the generation and transmission of indirect combustion noise through nozzles and ducts. For this reason, it is still used by some investigators today. However, the short nozzle approximation is primarily a one-dimensional approximation. It applies only to low frequency sound with wavelength longer than the nozzle length. Nowadays, the full Euler equations plus the energy equation can readily be solved computationally, at least, for geometrically simple laboratory experiments. The situation in real turbomachinery still presents a challenge. However, it is believed that for indirect combustion noise prediction, as well as for turbine attenuation of direct combustion noise, an effort should be made to use computational methods. This will ultimately allow a high-accuracy prediction over a much larger range of frequencies than the actuator-disk methods provide.

To predict indirect combustion noise from an engine, conventional thinking suggests that one should start with the prediction of the creation of hot and cold spots inside the combustor. Then the computation should follow the downstream convection of these entropy spots by the mean flow. Upon exiting the combustor, the flow carrying the entropy disturbances enters and makes its way through the high-pressure turbine. There is a general consensus that it is in the passage through the high-pressure turbine that significant amount of indirect combustion noise is generated. If this prediction strategy is followed then the prediction of indirect combustion noise from an engine is burdened with the need to first solve the combustor problem. Solving the combustor problem is by no means an easy task. It is, in many ways, more difficult than computing the generation of indirect combustion noise during the passage of entropy waves through a high-pressure turbine. For this reason, most recently some investigators, Tam and Parrish [121] and Papadogiannis et al. [122] tried to follow an alternative strategy. Their idea is to use a simplified entropy wave field as input to the nozzle or turbine flow computation. In both studies, a sinusoidal entropy wave train was used as input. This, of course, is an oversimplification of a real entropy wave field so their computation only yields qualitative results.

Earlier, Tam in his computational aeroacoustics book [123, Appendix F] presented an energy conserving method for discretizing a given pressure spectrum and then using the discretized information to create computationally a stochastic pressure wave field in the time domain. This method, when properly implemented, automatically ensures that the stochastic wave field created numerically has the same spectrum as the originally given pressure spectrum. Recently, this method was modified by Tam et al. [124] to generate a stochastic entropy wave field inside a Honeywell TECH977 engine. The spectrum in black shown in Fig. 2.4 is the spectrum computed by them using the modified Tam's method. The prescribed spectrum of their computed entropy wave field was the Schuster et al. [119] spectrum shown in orange color in Fig. 2.4. It is obvious that there is excellent agreement. The Tam method was originally formulated for plane waves. Most recently, the method has been extended to produce a fully three dimensional stochastic entropy-wave field in the time domain. In the extended method, two two-point spatial cross-correlation functions in two orthogonal directions in the lateral plane (plane perpendicular to the flow direction) are additional input functions. These cross-correlation functions allow a user to specify the lateral dimensions of the entropy blobs in the entropy wave field. In other words, if the extended method is used, a user can create a random broadband entropy wave field with a prescribed spectral shape and intensity in temperature fluctuations and distributions of the lateral dimensions of the entropy blobs through the specification of the lateral spatial cross-correlation functions.

Now, if the temperature fluctuation spectrum and the two-point cross-correlation functions are measured at a location slightly downstream of the combustor exit, it is possible through the use of the stochastic entropy wave field generation method to convert the measured data into a time domain inflow boundary condition for the computation of indirect combustion noise generation inside an engine or across a high-

pressure turbine. Such a boundary condition effectively replaces the engine combustor. In this way, the need to solve the combustor problem can be entirely circumvented. A significant benefit of this approach is also that the computed broadband noise is essentially indirect combustion noise. There is no need to carry out a noise component separation operation.

This alternative strategy was employed by Tam et al. [124] in their attempt to show that the noise increase across the high-pressure turbine inside the Honeywell TECH977 engine (see Fig. 2.5) is indirect combustion noise. To avoid full modeling of the turbines, they replaced the turbines by body forces with a magnitude such that the same pressure drops across the turbines as measured are reproduced. There is no tunable parameter in their computation. The computed results yielded a spectrum that matched well (within 3 dB) with the green spectrum in Fig. 2.5 up to about 1 kHz frequency. Above 1 kHz, the computed spectrum drops off rapidly. Tam et al. attributed the high frequency drop-off to the lack of details in their turbine model. So, a confirmation of the generation of indirect combustion noise in an engine is still lacking though some progress seems have been made.

Many investigators use numerical simulations to study and to predict indirect combustion noise generation inside an engine. A popular way is to employ a readily available commercial CFD code that the investigator had used before. But one must be cautioned that this may not be a good practice. The magnitude of sound inside an engine (except for resonance) is, in general, many orders of magnitude smaller than that of the fluid flow. The numerical noise of a commercial code may be tolerable for flow computation, but it could be comparable in level to that of indirect combustion noise. In addition, most commercial CFD codes have strong built-in numerical damping (because of numerical stability considerations). There is usually no simple way to assess the amount of damping or a way to alter the damping rate. Such damping could be strong enough to wipe out a big part of internally generated acoustic waves. To compute indirect combustion noise in an engine, it is natural to take the computational domain to be the entire flow path inside the engine. This choice, invariably, create inflow and outflow boundaries that require proper boundary conditions. The inflow boundary condition has to play a dual role. That is, it must generate the incoming entropy waves and at the same time allow the outgoing disturbances created inside the engine to exit without significant reflections. If an aeroacoustic code instead of a CFD code is employed for the time marching computation, a split-variable method (see Tam [123, Chapter 9]) could be used. At the outflow boundary, an absorbing boundary condition is needed to avoid contaminating the computed solution by wave reflected back by the outflow boundary back into the computational domain. Acoustic boundary conditions of these types are usually not a part of a commercial CFD code.

At this time, there is no clear experimental evidence that indirect combustion noise plays an important role in the noise produced by current generation aircraft engines. This does not mean that engines do not produce indirect combustion noise. This is, perhaps, because the intensity is relatively low and hence it is difficult to identify indirect combustion noise from all the other noise components emitted from an engine. Also we need better noise component separation methods to identify indirect combustion noise.

Part 3. High-Fidelity Simulations (Direct and Indirect Combustion Noise)

Predicting combustion noise is often done using semi-empirical methods, based on extrapolations and simplifications. The recent revolution due to the new performances of Large Eddy Simulation methods allows now to imagine that a fully deterministic simulation chain may be developed to predict combustion noise from first principle computations only [9, 125, 126]. The challenge is clearly a difficult one: it requires the simulation of the unsteady flow in combustion chambers and in turbine stages, followed by a jet noise simulation. Moreover, all these computations must be coupled: the LES of the combustion chamber must capture acoustic (direct noise) and entropy as well vorticity waves (indirect noise) and feed them to a tool computing the propagation of these waves in the rotor/stator stages; finally these perturbations must be introduced in a simulation of jet noise and propagated to the far field. A few groups

are trying to build such a chain using high-fidelity solvers and Fig. 3.1 displays an example of combustion noise prediction tool developed and applied to helicopter and aircraft noise in 2016 [127].

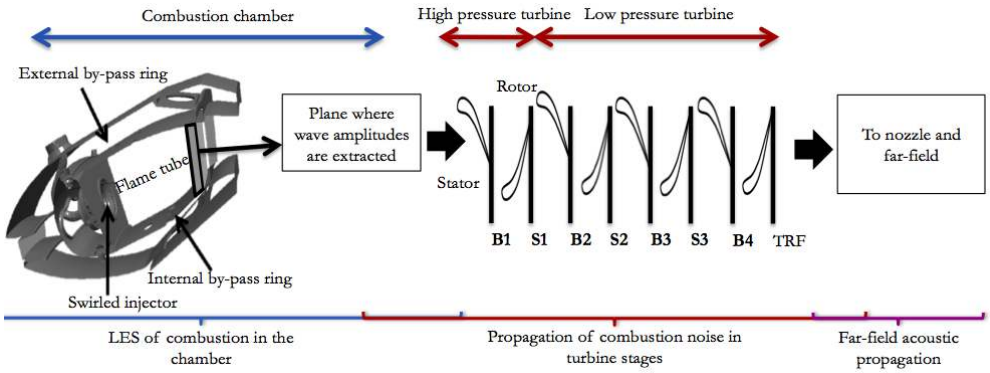

Fig. 3.1 A fully deterministic chain to compute combustion noise: LES is performed in the combustion chamber; acoustic, vorticity and entropy waves are measured at the combustor outlet plane and propagated into the turbine stages using actuator disk theory to obtain both direct and indirect noise in the outlet nozzle; a far field propagation tool is then used to propagate noise to the far field.

Using high-fidelity CFD methods for all components of Fig. 3.1 (combustion chamber, turbine, jet) remains impossible today. In the combustion chamber itself, LES has become the reference tool in the last ten years: recent progress in chemistry description and in turbulent subgrid scale models allows now to perform simulations of the unsteady reacting flow within chambers [128–130]. The chemical reactions controlling methane/air or kerosene/air flames can now be introduced in 3-D codes using tabulation methods or reduced chemistry approaches [131] while the flame/turbulence interaction is handled using sophisticated multiscale approaches zooming in the flame front to resolve its structure [128]. These simulations capture the unsteady motions of the flame front where heat release takes place, leading to strong flow divergence and direct noise production. However, even though LES can be used for the combustion chamber to predict all unsteady activity due to turbulence and combustion with precision, the situation is different in the turbine where it is much more difficult to use a high-fidelity method to predict noise propagation and generation by indirect mechanisms. In addition, the noise generated in the chamber and propagated through the turbine, must then be added to the computation of the jet noise before propagating to the far field. A reasonable compromise (displayed in Fig. 3.1) is to use LES in the combustion chamber and extract acoustic, vorticity and entropy waves at the outlet of the chamber, upstream of the first turbine stages. An analytical theory based on actuator-disk assumptions, can then be used to compute direct and indirect noise through the turbine stage. This requires the knowledge of the flow cross sections in the turbine and of the enthalpy jumps at each rotor but this is much cheaper than a full 3-D LES of the whole turbine. A limitation of actuator-disk theory is that the Marble and Cumpsty approach [104] used to describe wave propagation through a turbine stage is valid only for low frequencies (compact limit) where jump conditions can be written on both sides of the stage. Extending this theory to higher frequencies remains a challenge: this has been done already for simple nozzles where the Marble and Candel technique [3] valid too only under the compact assumption, has been extended to all one-dimensional waves by Durán and Moreau [132] using a Markus expansion. For a turbine stage with rotation effects, this remains to be done.

The most complete example of application of the tool described in Fig. 3.1 was given in 2016 [127] for a helicopter engine where such a prediction chain was used and compared to measurements performed by SAFRAN HELICOPTER ENGINES within the European TEENI project where sound levels were measured both inside and outside a real engine. Fig. 3.2 displays the engine geometry and shows where

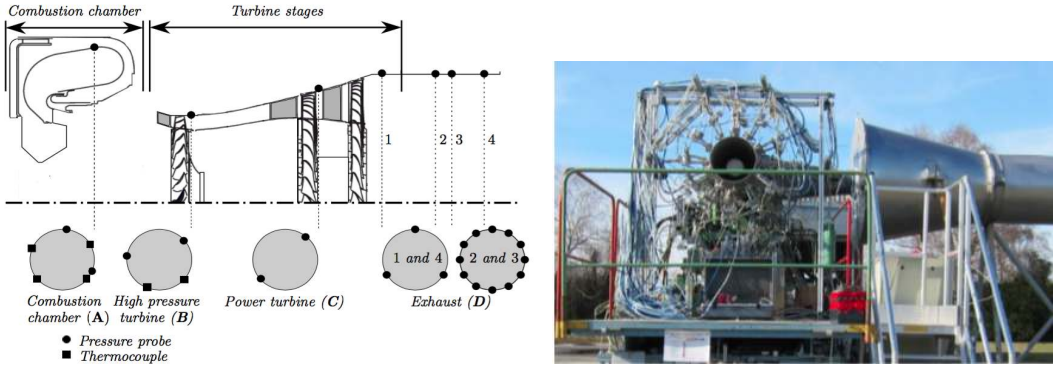

Fig. 3.2 The TEENI engine used to validate the computation chain of Fig. 3.1 [127].

pressure probes were used to measure sound within the combustor and the turbine. In addition, sound was also measured in the far field as shown on Fig. 3.3.

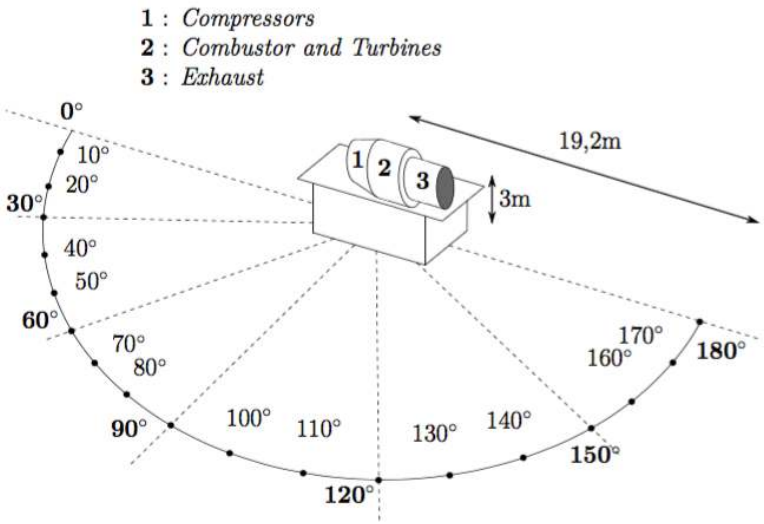

Fig. 3.3 Far field microphones used for the TEENI engine [127].

As soon as the objective is to compute the noise of a full annular chamber, the question of azimuthal modes and of the necessity of performing a full 360 degrees LES appears. Here, both single sectors and a full 360 degrees LES were performed. Results showed a limited impact of the azimuthal modes and a cancellation effect of noise between sectors: each burner generates noise which is not phased with the others so that the overall noise is not the simple addition of individual burner noise: a simple filtering method was developed to account for this cancellation effect. This filtering effect is mainly applied to entropy waves because indirect noise is the dominating noise generation mechanims in this engine. Noise levels were compared within the turbine and in the far field showing that the overall simulation chain of Fig. 3.1 has the potential to predict combustion noise in real engines (Fig. 3.4).

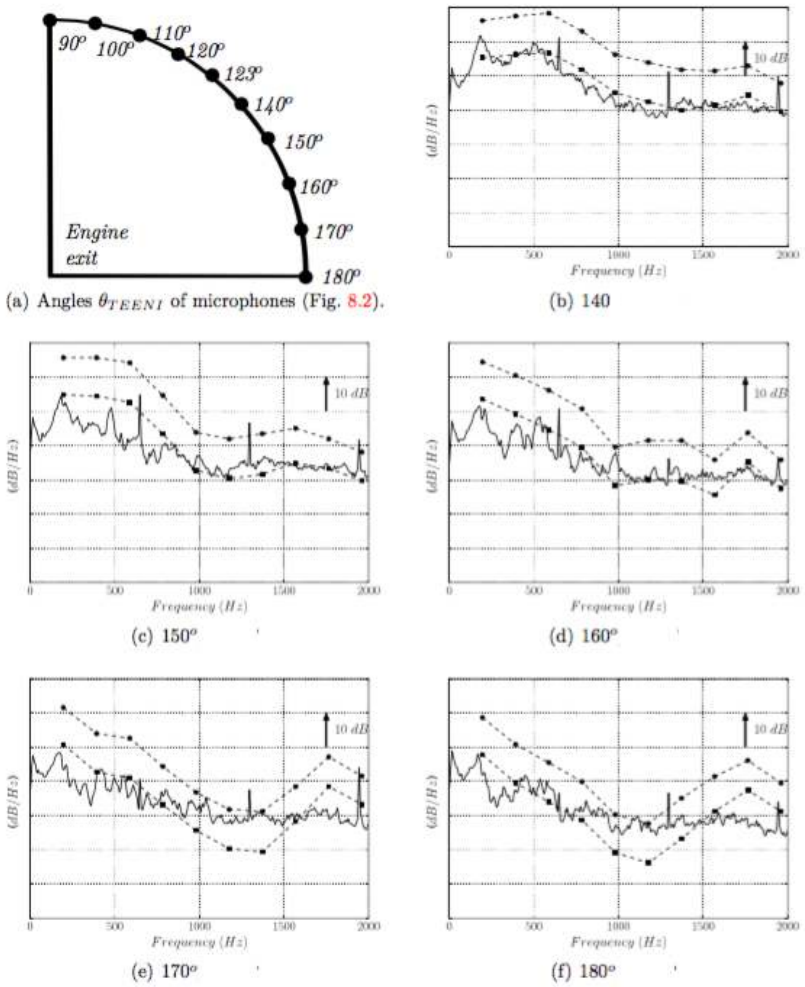

(a) Angles θ_{TEENI} of microphones (Fig. 8.2).
(b) 140
(c) 150°
(d) 160°
(e) 170°
(f) 180°

Fig. 3.4 Acoustic pressure from 140 degrees to 180 degrees in the far-field. The squares correspond to the LES results without entropy filtering and the circles to LES with filtering. Solid line: experimental data [127].

Acknowledgements L. S. Hultgren was supported by the NASA Advanced Air Vehicles Program, Advanced Air Transport Technology Project, Aircraft Noise Reduction Subproject.

References

1. L. S. Hultgren. A comparison of combustor-noise models. AIAA Paper 2012-2087 (NASA/TM-2012-217671), 18th AIAA/CEAS Aerocoustics Conference, Colorado Springs, Colorado, 2012.
2. S. M. Candel. *Analytical Studies of Some Acoustics Problems of Jet Engines*. PhD thesis, California Institute of Technology (Also DOT-TST-76-104 1976), 1972.
3. F. E. Marble and S. M. Candel. Acoustic disturbances from gas non-uniformities convected through a nozzle. *J. Sound and Vibration*, 55(2):225–243, 1977.
4. F. Bake, N. Kings, A. Fisher, and I. Röhle. Experimental investigation of the entropy noise mechanism in aero-engines. *International J. Aeroacoustics*, 8(1-2):125–142, 2009.

5. R. J. Mahan and A. Karchmer. Combustion and core noise. In H. H. Hubbard, editor, *Aeroacoustics of Flight Vehicles: Theory and Practice*, volume 1, chapter 9, pages 483–517. NASA Reference Publication 1258, WRDC Technical Report 90-3052, 1991.
6. S. Candel, D. Durox, S. Ducruix, A.-L. Birbaud, N. Noiray, and T. Schuller. Flame dynamics and combustion noise: Progress and challenges. *International J. Aeroacoustics*, 8(1&2):1–56, 2009.
7. I. Duran, S. Moreau, F. Nicoud, T. Livebardon, E Bouty, and T. Poinsot. Combustion noise in modern aero-engines. *Aerospace Lab Journal*, 7-05:1–11, (DOI: 10.12762/2014.AL07–05), 2014.
8. A. P. Dowling and Y. Mahmoudi. Combustion noise. *Proceedings of the Combustion Institute*, 35: 65–100, 2015.
9. M. Ihme. Combustion and engine-core noise. *Annual Review of Fluid Mechanics*, 49:277–310, 2017.
10. R.B. Price, I.R. Hurle, and T.M. Sugden. Optical studies of the generation of noise in turbulent flames. In *Twelfth Symposium (International) on Combustion: At the University of Poitiers, France, July, 1968*, pages 1093–1102. Proceedings of the Combustion Institute, 1969.
11. I. R. Hurle, R. B. Price, T. M. Sugden, and A. Thomas. Sound emission from open turbulent premixed flames. *Proc. Roy. Soc. A*, 303(1475):409–427, 1968.
12. B. N. Shivashankara, W. C. Strahle, and J. C. Handley. Evaluation of combustion noise scaling laws by an optical technique. *AIAA J.*, 13(5):623–627, 1975.
13. S. Bragg. Combustion noise. *J. Inst. Fuel*, 36(1):12–16, 1963.
14. T. J. B. Smith and J. K. Kilham. Noise generation by open turbulent flames. *J. Acoustical Society of America*, 35(5):715–724, 1963.
15. A. Thomas and G. T. Williams. Flame noise: Sound emission from spark-ignited bubbles of combustible gas. *Proc. Roy. Soc. A*, 294(1439):449–466, 1966.
16. D. I. Abugov and O. I. Obrezkov. Acoustic noise in turbulent flames. *Combustion, Exposion and Shock Waves*, 14(5):606–612, 1978.
17. P. Clavin and E. D. Siggia. Turbulent premixed flames and sound generation. *Combustion Science and Technology*, 78(1-3):147–155, 1991.
18. R. Rajaram and T. Lieuwen. Parametric studies of acoustic radiation from premixed flames. *Combustion Science and Technology*, 175:2269–2298, 2003.
19. C. Hirsh, J. Wäsle, A. Winkler, and T. Sattelmayer. A spectral model for the sound pressure from turbulent premixed combustion. *Proceedings of the Combustion Institute*, 31(1):1435–1441, 2007.
20. W. C. Strahle. On combustion generated noise. *J. Fluid Mech.*, 49:399–414, 1971.
21. W. C. Strahle. Some results in combustion generated noise. *J. Sound and Vibration*, 23(1):113–125, 1972.
22. M. J. Lighthill. On sound generated aerodynamically. I. General theory. *Proc. R. Soc. Lond. A*, 211 (1107):564–587, 1952. doi: 10.1098/rspa.1952.0060.
23. M. J. Lighthill. On sound generated aerodynamically. II. Turbulence as a source of sound. *Proc. R. Soc. Lond. A*, 222(1148):1–32, 1954. doi: 10.1098/rspa.1954.0049.
24. C. K. W. Tam, K. Viswanathan, K. K. Ahuja, and J. Panda. The sources of jet noise: Experimental evidence. *J. Fluid Mech.*, 615:235–292, 2008.
25. C. Bailly, C. Bogey, and S. Candel. Modelling of sound generation by turbulent reacting flows. *International J. Aeroacoustics*, 9(4-5):461–490, 2010.
26. O. M. Phillips. On the generation of sound by supersonic turbulent shear layers. *J. Fluid Mech.*, 9 (1):1–28, 1960.
27. G. M. Lilley. The generation and radiation of supersonic jet noise. Technical Report AFAPL-TR-72-53, Air Force Aero-Propulsion Laboratory, 1972.
28. G. M. Lilley. The source of aerodynamic noise. *International J. Aeroacoustics*, 2(3-4):241–254, 2003.

29. S. Kotake and K. Takamoto. Combustion noise: Effects of the shape and size of burner nozzle. *J. Sound Vibration*, 112(2):345–354, 1987.
30. R. Rajaram, Preetham, and T. Lieuwen. Frequency scaling of turbulent premixed flame noise. AIAA Paper 2005-2828, 11th AIAA/CEAS Aeroacoustics Conference, Monterey, California, 2005.
31. B. N. Shivashankara, W. C. Strahle, and J. C. Handley. Combustion noise radiated by open turbulent flames. In H. T. Nagamatsu, J. V. O'Keefe, and I. R. Schwartz, editors, *Aeroacoustics: Jet and Combustion Noise; Duct Acoustics*, volume 37 of *Progress in Astronautics and Aeronautics*, pages 277–296. AIAA, 1975.
32. R. N. Kumar. Further experimental results on the structure and acoustics of turbulent jet flames. In I. R. Schwartz, H. T. Nagamatsu, and W. C. Strahle, editors, *Aeroacoustics: Jet Noise, Combustion and Core Engine Noise*, volume 43 of *Progress in Astronautics and Aeronautics*, pages 483–507. AIAA, 1976.
33. J. K. Kilham and N. Kirmani. The effect of turbulence on premixed flame noise. In *Seventeenth Symposium (International) on Combustion, Leeds, England, 1979*, pages 327–336. Proceedings of the Combustion Institute, 1979.
34. S. Kotake and K. Takamoto. Combustion noise: Effects of the velocity turbulence of unburned mixture. *J. Sound and Vibration*, 139(1):9–20, 1990.
35. N. Ohiwa, K. Tanaka, and S. Yamaguchi. Noise characteristics of turbulent diffusion flames with coherent structure. *Combustion Science and Technology*, 90(1-4):61–78, 1993.
36. P. R. Knott. Noise generated by turbulent non-premixed flames. AIAA Paper 1971-0732, AIAA/SAE 7th Propulsion Joint Specialist Conference, Salt Lake City, Utah, 1971.
37. W. C. Strahle. A review of combustion generated noise. AIAA Paper 1973-1023, AIAA Aero-Acoustics Conference, Seattle, Washington, 1973.
38. H. A. Hassan. Scaling of combustion-generated noise. *J. Fluid Mech.*, 66(3):445–453, 1974.
39. T. Lieuwen and R. Rajaram. Acoustic radiation from premixed flames subjected to convective flow disturbances. AIAA Paper 2002-0480, 40th AIAA Areospace Sciences Meeting, Reno, Nevada, 2002.
40. R. Rajaram and T. Lieuwen. Effect of approach flow turbulence characteristics on sound generation from premixed flames. AIAA Paper 2004-0461, 42nd AIAA Aerospace Sciences Meeting and Exhibit, Reno, Nevada, 2004.
41. T. J. B. Smith. *Combustion Noise*. PhD thesis, University of Leeds, 1961.
42. B. N. Shivashankara. *An Experimental Study of Noise Produced by Open Turbulent Flames*. PhD thesis, Georgia Institute of Technology, 1973.
43. T. Lieuwen, S. Mohan, R. Rajaram, and Preetham. Acoustic radiation from weakly wrinkled premixed flames. *Combustion and Flame*, 144(1-2):360–369, 2006.
44. A. A. Putnam. Combustion roar of seven industrial gas burners. *J. Inst. Fuel*, 49(400):135–138, 1976.
45. R. Rajaram and T. Lieuwen. Acoustic radiation from turbulent premixed flames. *J. Fluid Mechanics*, 637:357–385, 2009.
46. C. K. W Tam, N. N. Pastouchenko, J. Mendoza, and D Brown. Combustion noise of auxiliary power units. AIAA Paper 2005-2829, 11th AIAA/CEAS Aeroacoustics Conference, Monterey, California, 2005.
47. C. K. W. Tam, M. Golebiowski, and J. M. Seiner. On the two components of turbulent mixing noise from supersonic jets. Technical Report AIAA Paper 1996-1716, 2nd AIAA Aeroacoustics Conference, State College, Pensylvania, 1996.
48. C. K. W. Tam. The spectral shape of combustion noise. *International J. Aeroacoustics*, 14(3-4): 431–456, 2015. doi: http://doi.org/10.1016/j.jsv.2015.04.010.
49. W. C. Strahle. Combustion noise. *Prog. Energy and Combust. Sci.*, 4(3):157–176, 1978.

50. L. S. Hultgren, J. H. Miles, and P. C. E. Jorgenson. Engine system and core noise. In M. D. Dahl, editor, *Assessment of NASA's Aircraft Noise Prediction Capability*, chapter 3, pages 35–62. NASA/TP-2012-215653, 2012.
51. A. M. Karchmer. Acoustic modal analysis of a full scale annular combustor. AIAA Paper 1983-0760 (NASA-TM-83334), 8th AIAA Aeroacoustics Conference, Atlanta, Georgia, 1983.
52. C. M. Royalty and B. Schuster. Noise from a turbofan engine without a fan from the engine validation of noise and emission reduction technology (EVNERT) program. AIAA Paper 2008-2810, 14th AIAA/CEAS Aeroacoustics Conference, Vancouver, British Columbia, 2008.
53. E. A. Krejsa and A. M. Karchmer. Acoustic modal analysis of the pressure field in the tailpipe of a turbofan engine. Technical Report NASA-TM-83387, NASA, 1983.
54. B. Schuster and L. Lieber. Narrowband model for gas turbine engine combustion noise prediction. AIAA Paper 2006-2677, 12th AIAA/CEAS Aerocoustics Conference, Cambridge, Massachusetts, 2006.
55. R. Motsinger. Prediction of engine combustor noise and correlation with T64 engine low frequency noise. Technical Report R72AEG313, General Electric Co., 1972.
56. J. J. Emmerling, S. B. Kazin, and R. K. Matta. Core engine noise control program, Volume III, Supplement 1—Prediction methods. Technical Report FAA-RD-74-125 III-I (AD A030376), FAA, 1976.
57. D. C. Mathews, N. F. Rekos, Jr, and R. T. Nagel. Combustion noise investigation. Technical Report FAA-RD-77-3, FAA, 1977.
58. D. C. Mathews and N. F. Rekos, Jr. Prediction and measurement of direct combustion noise in turbopropulsion systems. *J. Aircraft*, 14(9):850–859, 1977.
59. P. Y. Ho and V. L. Doyle. Combustion noise prediction update. AIAA Paper 1979-0588, 5th AIAA Aerocoustics Conference, Seattle, Washington, 1979.
60. R. S. Zuckerman. Core engine noise reduction: Definition and trends. AIAA Paper 1977-1273, 4th AIAA Aeroacoustics Conference, Atlanta, Georgia, 1977.
61. Society of Automotive Engineers International. Gas turbine jet exhaust prediction. Technical Standard SAE ARP876 Rev. E, 2006.
62. W. E. Zorumski. Aircraft noise prediction program theoretical manual, part 1. Technical Report NASA-TM-83199-PT-1, NASA, 1982.
63. W. E. Zorumski. Aircraft noise prediction program theoretical manual, part 2. Technical Report NASA-TM-83199-PT-2, NASA, 1982.
64. R. E. Gillian. Aircraft noise prediction program user's manual. Technical Report NASA-TM-84486, NASA, 1982.
65. L. S. Hultgren. Full-scale turbofan-engine turbine-transfer function determination using three internal sensors. AIAA Paper 2011-2912 (NASA/TM-2012-217252), 17th AIAA/CEAS Aeroacoustic Conference, Portland, Oregon, 2011.
66. D. S. Weir. Engine validation of noise and emission reduction technology phase I. Technical Report NASA/CR-2008-215225, NASA, 2008. Honeywell Report No. 21-13843, Honeywell Aerospace, Phoenix, Arizona.
67. L. S. Hultgren and J. H. Miles. Noise-source separation using internal and far-field sensors for a full-scale turbofan engine. AIAA Paper 2009-3220 (NASA/TM–2009-215834), 15th AIAA/CEAS Aeroacoustic Conference, Miami, Florida, 2009.
68. L. Bertsch, S. Guérin, G. Looye, and M. Pott-Pollenske. The parametric aircraft noise analysis module - status overview and recent applications. AIAA Paper 2011-2855, 17th AIAA/CEAS Aeroacoustic Conference, Portland, Oregon, 2011.
69. L. Bertsch, W. Dobrzynski, and S. Guérin. Tool development for low-noise aircraft design. *J. Aircraft*, 47(2):694–699, 2010.

70. L. Bertsch and U. Isermann. Noise prediction toolbox used by the DLR aircraft noise working group. Paper, 42nd International Congress and Exposition on Noise Control Engineering (Inter-Noise 2013), Innsbruck, Austria, 2013.
71. M. Brunet, P. Malbéqui, and W. Ghedhaifi. A novel approach to air transport system environmental impact evaluation through physical modelling and simulation. Paper, 26th International Congress of the Aeronautical Sciences (ICAS'08), 2008.
72. L. Sanders, P. Malbéqui, and I. LeGriffon. Capabilities of IESTA-CARMEN to predict aircraft noise. ICSV23 Paper 255, 23rd International Congress on Sound & Vibration (ICSV23), Athens, Greece, 2016.
73. M. Brunet, T. Chaboud, N. Huynh, P. Malbéqui, and W. Ghedhaifi. Environmental impact evaluation of air transport systems through physical modelling and simulation. AIAA Paper 2009-6936, 9th AIAA Aviation Technology, Integration, and Operations Conference (ATIO), Hilton Head, South Carolina, 2009.
74. P. Gliebe, R. Mani, H. Shin, B. Mitchel, G. Ashford, S. Salamah, and S. Connell. Aeroacoustic prediction codes. Technical Report NASA/CR-2000-210244, NASA, 2000.
75. G. F. Pickett. Core engine noise due to temperature fluctuations convecting through turbine blade rows. AIAA Paper 1975-0528, 2nd AIAA Aero-Acoustics Conference, Hampton, Virginia, 1975.
76. F. Bake, U. Michel, I. Röhle, C. Richter, F. Thiele, M. Liu, and B. Noll. Indirect combustion noise generation in gas turbines. AIAA Paper 2005-2830, 11th AIAA/CEAS Aeroacoustics Conference, Monterey, California, 2005.
77. F. Bake, U. Michel, and I. Röhle. Investigation of entropy noise in aero-engine combustors. Paper GT2006-90093, ASME Turbo Expo 2006, Barcelona, Spain, 2006.
78. F. Bake, U. Michel, and I. Röhle. Experimental investigation of the fundamental entropy noise mechanism in aero-engines. AIAA Paper 2007-3694, 13th AIAA/CEAS Aeroacoustics Conference, Rome, Italy, 2007.
79. F. Bake, U. Michel, and I. Röhle. Fundamental mechanisms of entropy noise in aero-engines: Experimental investigation. Paper GT2007-27300, ASME Turbo Expo 2007, Montreal, Canada, 2007.
80. F. Bake, U. Michel, and I. Röhle. Investigation of entropy noise in aero-engine combustors. *J. Eng. Gas Turbines Power*, 129(2):370–376, 2007.
81. N. Kings and F. Bake. Indirect combustion noise: Noise generation by accelerated vorticity in a nozzle flow. *International J. Spray and Combustion Dynamics*, 2(3):253–266, 2010.
82. N. Kings, L. Enghardt, and F. Bake. Indirect combustion noise: Experimental investigation of the vortex sound generation in accelerated swirling flows. AIAA Paper 2013-2100, 19th AIAA/CEAS Aeroacoustic Conference, Berlin, Germany, 2013.
83. N. Kings, L. Enghardt, and F. Bake. Broadband indirect noise generation by accelrated vorticity. AIAA Paper 2015-2820, 21st AIAA/CEAS Aeroacoustic Conference, Dallas, Texas, 2015.
84. A. Fischer, F. Bake, and I. Röhle. Broadband entropy noise phenomena in a gas turbine combustor. Paper GT2008-50263, ASME Turbo Expo 2008, Berlin, Germany, 2008.
85. B.-T. Chu and L. S. G. Kovasznay. Non-linear interactions in a viscous heat-conducting compressible gas. *J. Fluid Mech.*, 3:494–514, 1958.
86. C. K. W Tam and S. A. Parrish. On the generation of indirect combustion noise. AIAA Paper 2014-3315, 20th AIAA/CEAS Aeroacoustics Conference, Atlanta, Georgia, 2014.
87. E. E. Zukoski and J. M. Auerbach. Experiments concerning the response of supersonic nozzles to fluctuating inlet conditions. *J. Engineering for Power*, 98(1):60–64, 1976.
88. M. S. Bohn. Responce of a subsonic nozzle to acoustic and entropy disturbances. *J. Sound and Vibration*, 52(2):283–297, 1977.
89. W. C. Strahle and M. Muthukrishnan. Correlation of combustor rig sound power data and theoretical basis of results. *AIAA J.*, 18(3):269–274, 1980.

90. M. Muthukrishnan, W. C. Strahle, and D. H. Neale. Separation of hydrodynamic, entropy, and combustion noise in a gas turbine combustor. *AIAA J.*, 16(4):320–327, 1978.
91. A. Guédel and A. Farrando. Experimental study of turboshaft engine core noise. *J. Aircraft*, 23(10): 763–767, 1986.
92. F. Bake, N. Kings, A. Fischer, and I. Röhle. Indirect combustion noise: Investigations of noise generated by the acceleration of flow inhomogeneities. *Acta Acustica United with Acustica*, 95: 461–469, 2009.
93. F. Bake, C. Richter, B. Mühlbauer, N. Kings, I. Röhle, F. Thiele, and B. Noll. The entropy wave generator (ewg): A reference case on entropy noise. *J. Sound and Vibration*, 326((3-5)):574–598, 2009.
94. M. Leyko, F. Nicoud, and T. Poinsot. Comparison of direct and indirect combustion noise mechanisms in a model combustor. *AIAA J.*, 47(11):2709–2716, 2009.
95. M. Leyko, S. Moreau, F. Nicoud, and T. Poinsot. Wave transmission and generation in turbine stages in a combustion-noise framework. AIAA Paper 2010-4032, 16th AIAA/CEAS Aerocoustics Conference, Stockholm, Sweden, 2010.
96. I. Durán and S. Moreau. Analytical and numerical study of the entropy wave generator experiment on indirect combustion noise. AIAA Paper 2011-2829, 17th AIAA/CEAS Aeroacoustic Conference, Portland, Oregon, 2011.
97. C. S. Goh and A. S. Morgans. Phase prediction of the responce of choked nozzles to entropy and acoustic disturbances. *J. Sound and Vibration*, 330(21):5184–5198, 2011.
98. A. Giauque, M. Huet, and F. Clero. Analytical analysis of indirect combustion noise in subcritical nozzles. *J. Eng. Gas Turbines Power*, 134(11):111202–1–8, 2012.
99. A. S. Morgans, C. S. Goh, and J. A. Dahan. The dissipation and shear dispersion of entropy waves in combustor thermoacoustics. *J. Fluid Mech. (JFM Rapids)*, 733:R2–1–11, 2013.
100. M. Leyko, S. Moreau, F. Nicoud, and T. Poinsot. Numerical and analytical modelling of entropy noise in a supersonic nozzle with a shock. *J. Sound and Vibration*, 330(16):3944–3958, 2011.
101. I. Durán and S. Moreau. Study of the attenuation of waves propagating through fixed and rotating turbine blades. AIAA Paper 2012-2133, 18th AIAA/CEAS Aerocoustics Conference, Colorado Springs, Colorado, 2012.
102. I. Durán and S. Moreau. Numerical simulation of acoustic and entropy waves propagating through turbine blades. AIAA Paper 2013-2102, 19th AIAA/CEAS Aeroacoustic Conference, Berlin, Germany, 2013.
103. A. Mishra and D. J. Bodony. Evaluation of actuator disk theory for predicting indirect combustion noise. *J. Sound and Vibration*, 332(4):821–838, 2013.
104. N. A. Cumpsty and F. E. Marble. The interaction of entropy fluctuations with turbine blade rows; a mechanism of turbojet engine noise. *Proc. R. Soc. Lond. A*, 357:323–344, 1977.
105. C. S. Goh and A. S. Morgans. The infuence of entropy waves on the thermoacoustic stability of a model combustor. *Combustion Science and Technology*, 185(2):249–268, 2013.
106. C. K. W Tam, S. A. Parrish, J. Xu, and B. Schuster. Indirect combustion noise of auxiliary power units. *J. Sound and Vibration*, 332:4004–4020, 2013.
107. K. Knobloch, T. Werner, and F. Bake. Entropy noise generation and reduction in a heated nozzle flow. AIAA Paper 2015-2818, 21st AIAA/CEAS Aeroacoustic Conference, Dallas, Texas, 2015.
108. J. H. Miles. Time delay analysis of turbofan engine direct and indirect combustion noise sources. *J. Propulsion and Power*, 25(1):218–227, 2009.
109. J. H. Miles. Separating direct and indirect engine combustion noise using the correlation function. *J. Propulsion and Power*, 26(5):1144–1152, 2010.
110. F. Bake, P. Gaetani, G. Persico, L. Neuhaus, and K. Knobloch. Indirect noise generation in a high pressure turbine stage. AIAA Paper 2016-3004, 22nd AIAA/CEAS Aeroacoustic Conference, Lyon, France, 2016.

111. B. Pardowitz, U. Tapken, K. Knobloch, F. Bake, E. Bouty, I. Davis, and G. Bennett. Core noise — identification of broadband noise sources of a turbo-shaft engine. AIAA Paper 2014-3321, 20th AIAA/CEAS Aeroacoustics Conference, Atlanta, Georgia, 2014.
112. J. Y. Chung. Rejection of flow noise using a coherence function method. *J. Acoustical Society of America*, 62(2):388–395, 1977.
113. J. S. Hsu and K. K. Ahuja. A coherence-based technique to separate internal mixing noise from farfield measurements. AIAA Paper 1998-2296, 4th AIAA/CEAS Aeroacoustic Conference, Toulouse, France, 1998.
114. T. Minami and K. K. Ahuja. Five microphone method for separating two different noise sources from farfield measurements contaminated by extraneous noise. AIAA Paper 2003-3261, 9th AIAA/CEAS Aeroacoustic Conference, Hilton Head, South Carolina, 2003.
115. I. Davis and G. J. Bennett. Experimental investigations of coherence based noise source identification techniques for turbomachinery applications - classic and novel techniques. AIAA Paper 2011-2830, 17th AIAA/CEAS Aeroacoustic Conference, Portland, Oregon, 2011.
116. I. Davis and G. J. Bennett. Spatial noise source identification of tonal noise in turbomachinery using the coherence function on a modal basis. AI 2011-2825, 17th AIAA/CEAS Aeroacoustic Conference, Portland, Oregon, 2011.
117. L. Enghardt, A. Holewa, and U. Tapken. Comparison of different analysis techniques to decompose a broad-band ducted sound field in its mode constituents. AIAA Paper 2007-3520, 13th AIAA/CEAS Aeroacoustics Conference, Rome, Italy, 2007.
118. W. Jürgens, U. Tapken, B. Pardowitz, P. Kausche, G. J. Bennett, and L. Enghardt. Technique to analyze characteristics of turbomachinery broadband noise sources. AIAA Paper 2010-3979, 16th AIAA/CEAS Aerocoustics Conference, Stockholm, Sweden, 2010.
119. B. Schuster, G. Gordon, and L. S. Hultgren. Dynamic temperature and pressure measurements in the core of a propulsion engine. AIAA Paper 2015-2819, 21st AIAA/CEAS Aeroacoustic Conference, Dallas, Texas, 2015.
120. N. A. Cumpsty and F. E. Marble. Core noise from gas turbine exhausts. *J. Sound and Vibration*, 54 (2):297–309, 1977.
121. C. K. W. Tam and S. A. Parrish. Noise of high-performance aircraft at afterburner. *J. Sound and Vibration*, 352:103–128, 2015.
122. D. Papadogiannis, G. Wang, S. Moreau, F. Duchaine, L. Gicquel, and F. Nicoud. Assessment of the indirect combustion noise generated in a transonic high-pressure turbine stage. *J. Eng. Gas Turbines Power*, 138(4):041503–1–8, 2016.
123. C. K. W. Tam. *Computational Aeroacoustics: A Wavenumber Approach*. Cambridge University Press, 2012.
124. C. K. W Tam, Z Li, and B. Schuster. An investigation on indirect combustion noise generation in a turbofan engine. AIAA Paper 2016-2746, 22nd AIAA/CEAS Aeroacoustic Conference, 2016.
125. M. Leyko, I. Durán, S. Moreau, F. Nicoud, and T. Poinsot. Simulation and modelling of the waves transmission and generation in a stator blade row in a combustion-noise framework. *J. Sound and Vibration*, 333(23):6090–6106, 2014.
126. I. Durán, S. Moreau, and T. Poinsot. Analytical and numerical study of combustion noise through a subsonic nozzle. *AIAA J.*, 51(1):42–52, 2013.
127. T. Livebardon, S. Moreau, L. Gicquel, T. Poinsot, and E. Bouty. Combining les of combustion chamber and an actuator disk theory to predict combustion noise in a helicopter engine. *Combustion and Flame*, 165:272–287, 2016.
128. T. Poinsot and D. Veynante. *Theoretical and Numerical Combustion*. elearning.cerfacs.fr/combustion, third edition, 2012.
129. H. Pitsch. Large-eddy simulation of turbulent combustion. *Annual Review of Fluid Mechanics*, 38: 453–482, 2006.

130. T. Poinsot. Prediction and control of combustion instabilities in real engines. *Proceedings of the Combustion Institute*, 36(1):1–28, 2017.
131. T. Jaravel, E. Ribner, B. Cuenot, and G. Bulat. Large eddy simulation of a model gas turbine burner using reduced chemistry with accurate pollutant prediction. *Proceedings of the Combustion Institute*, 36(3):3817–3825, 2017.
132. I. Durán and S. Moreau. Solution of the quasi-one-dimensional linearized Euler equations using flow invariants and the Magnus expansion. *J. Fluid Mech.*, 723:190–231, 2013.